

**Thesis**

**On**

**“STUDY THE TEMPERATURE DEPENDENT PERFORMANCE ANALYSIS OF  
MULTILAYER GRAPHENE NANORIBBON (MLGNR) AS VLSI  
INTERCONNECT”**

Submitted towards the partial fulfillment of requirement for the award of degree of

**Master of Technology**

**In**

**VLSI Design**

**Submitted by:**

**Surbhi**

Roll No: 601562026

**Under the guidance of**

**Dr. Mayank Kumar Rai**

Assistant Professor



**ELECTRONICS AND COMMUNICATION ENGINEERING**

**DEPARTMENT**

**THAPAR UNIVERSITY**

**(Established under the section 3 of UGC Act, 1956)**

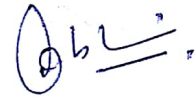
**PATIALA – 147004 (PUNJAB)**

July 2017

## DECLARATION

I, SURBHI SHARDA hereby declare that the work presented in this thesis entitled “**STUDY THE TEMPERATURE DEPENDENT PERFORMANCE ANALYSIS OF MULTILAYER GRAPHENE NANORIBBON (MLG NR) AS VLSI INTERCONNECT**” in partial fulfillment of the requirement for the award of degree of Master of Technology submitted at Electronics and Communication Engineering Department, Thapar University, Patiala is an authentic record of work carried out under supervision of Dr. Mayank Kumar Rai (Assistant Professor, ECED, Thapar University, Patiala). The matter presented in this has not been submitted either in part or full to any other university or institute for the award of any other degree.

Date: 21/08/2017



SURBHI SHARDA

Roll No. 601562026

It is certified that the above statement made by the candidate is correct to the best of my knowledge and belief.

Date: 21/08/2017



Dr. Mayank Kumar Rai

Assistant Professor

ECED, TU, Patiala

## **ACKNOWLEDGEMENT**

This report has only been possible with the constant guidance and expertise of Dr. Mayank Kumar Rai, Assistant Professor, Electronics and Communication Engineering Department, Thapar University, Patiala and I would like to take this opportunity to express my sincere gratitude to him.

I am also thankful to Dr. Alpana Agarwal, Head of ECE Department, for providing us the adequate infrastructure for carrying out the work.

I am also thankful to Dr. Hem Dutt Joshi, PG Coordinator as well as Dr. Anil Arora, Program Coordinator and the entire faculty and staff of Electronics and Communication Engineering Department for the motivation and inspiration that triggered me for the work.

I would also like to thank my friends who always motivated me and have more or less contributed to the preparation of this report. I will be always indebted to them.

Last but not the least, I would like to thank my parents for their years of unyielding love and encourage. They have always wanted the best for me and I admire their determination and sacrifice.

## ABSTRACT

---

As the technology is evolving the performance of interconnects in a circuit that was once neglected, is now turning out to be major concern for the high performance integrated circuits. It has been realized that with the scaling of technology in deep submicron (DSM) region, the resistance of consistently used copper (Cu) interconnects has started to increase due to surface roughness and grain boundary scattering. However, the resistance and capacitance play an important role in determining the performance of interconnects in terms of propagation delay, power dissipation and crosstalk. Due to continuous scaling of technology, the high performance circuits are becoming highly sensitive to temperature variations. Therefore, temperature is turning out to be one of the major factors that determine the performance of an interconnect material. The allotropes of carbon such as Carbon nano tubes (CNTs) and Graphene nanoribbons (GNRs) are being recommended as next generation interconnect materials to reduce the performance limiting factor like power, PDP, delay and the crosstalk noise voltage in VLSI interconnects.

This thesis work briefly presents the temperature dependent modeling and performance analysis of multilayer graphene nanoribbons (MLGNRs) based interconnects. The temperature dependent performance analysis is done, using SPICE simulations, in terms of propagation delay, power dissipation, frequency spectrum of the output pulse, crosstalk induced noise voltage and its frequency spectrum for MLGNR interconnects at 14nm technology node. A comparative performance analysis is done between MLGNR and conventionally used copper interconnects over a temperature range from 300K to 500K at 14nm technology node. According to the results, with the rise in temperature from 300K to 500K, the performance of MLGNR is superior as compared to copper interconnects.

Also the performance comparison is done between the temperature independent model of MLGNR with the temperature dependent model. The simulation results reveal that the delay and power dissipation of MLGNR, obtained through temperature dependent model are lower as compared to conventionally (temperature-independent) used model of MLGNR, at different interconnect lengths from 400 $\mu$ m to 1000 $\mu$ m. Also the results gives the effect of temperature on the frequency spectrum of MLGNR interconnects. It is found that the increase in temperature cause the loss in signal power and decrease in bandwidth.

Further the time duration of victim output waveform of temperature dependent model of MLGNR is compared with that of temperature independent model at different interconnect

lengths, ranging from 400  $\mu\text{m}$  to 1000 $\mu\text{m}$ . An average improvement of 38.9% is noticed in the time duration of temperature dependent model of MLGNR when compared with temperature independent model. Therefore, it is important to take temperature-dependent models into consideration for the performance optimization of high speed integrated circuits. Also, the performance superiority of MLGNR compared to copper based interconnects at 14nm technology, makes it a possible replacement for copper based interconnects in deep submicron (DSM) region.

# TABLE OF CONTENTS

---

	PAGE NO.
DECLARATION	ii
ACKNOWLEDGEMENT	iii
ABSTRACT	iv
LIST OF ACRONYMS	x
LIT OF FIGURES	xi
LIST OF TABLES	xiv
LIST OF SYMBOLS	xv
<b>CHPATER 1: INTERODUCTION AND STATEMENT OF THE PROBLEMS</b>	1
1.1 Interconnects	1
1.1.1 Why, Allotropes Of Carbon Are Being Recommended As Next Generation Interconnect Materials.	1
1.2 Graphene Nano-Ribbon (GNR)	3
1.2.1 GNRs Properties	3
1.2.2 Types Of GNRs	3
1.2.3 Performance Comparison Of GNR With Other Materials	5
1.3 Statement Of The Problems	5
1.4 Organization Of The Thesis	6

<b>CHAPTER 2: LITERATURE SURVEY</b>	8
2.1 Introduction	8
2.2 Literature review	8
2.3 Conclusion	13
<b>CHAPTER 3: TEMPERATURE DEPENDENT CIRCUIT MODELING OF MLGNR INTERCONNECTS</b>	14
3.1 Introduction	14
3.2 Temperature Dependent And Independent Modelling Of MLGNR	14
3.2.1 Temperature Dependent Modeling Of MLGNR	15
3.3 RLC Modeling For Copper Interconnects	22
3.4 Conclusion	23
<b>Chapter 4: PERFORMANCE ANALYSIS OF MLGNR INTERCONNECTS</b>	24
4.1 Introduction	24
4.2 Impedance Analysis	25
4.3 Performance Analysis	28
4.3.1 Delay Analysis	29
4.3.2 Power Analysis	30

4.3.3	Power Delay Product (PDP)	31
4.3.4	Frequency Spectrum Analysis	32
4.4	Conclusion	34
<b>CHAPTER 5: CROSSTALK ANALYSIS</b>		35
5.1	Introduction	35
5.2	Crosstalk Analysis	35
5.3	Frequency Spectrum Analysis	38
5.4	Conclusion	39
<b>CHAPTER 6: A COMPARATIVE ANALYSIS BETWEEN MLG NR AND COPPER BASED INTERCONNECTS</b>		40
6.1	Introduction	40
6.2	Performance Analysis And Comparison Of Copper Based Interconnects	40
6.2.1	Delay Analysis	41
6.2.2	Power Dissipation Analysis	41
6.2.3	Power Delay Product (PDP) Analysis	42
6.2.4	Frequency Spectrum Analysis	43
6.2.5	Crosstalk Analysis	44
6.2.6	Frequency Spectrum Analysis	46

6.3 Conclusion	47
<b>CHAPTER 7: CONCLUSION AND FUTURE SCOPE</b>	48
7.1 Introduction	48
7.2 Summary	48
7.3 Future Scope	50
<b>REFERENCES</b>	51

## LIST OF ACRONYMS

---

ac-GNR	Armchair Graphene Nano-ribbon
CNT	Carbon Nanotube
CMOS	Complementary Metal Oxide Semiconductor
DSM	Deep Sub-Micron
EDP	Energy Delay Product
ESC	Equivalent Single Conductor
GHz	Giga Hertz
GNR	Graphene Nano-ribbon
IC	Integrated Circuit
ITRS	International Technology Roadmap for Semiconductor
MFP	Mean Free Path
MCB	Mixed Carbon-nanotube Bundle
MWCNT	Multi Walled Carbon Nanotube
MLGNR	Multi-Layer Graphene Nano-ribbon
PDP	Power Delay Product
RLC	Resistance-Inductance- Capacitance
SC-MLGNR	Side Contact Multi-Layer Graphene Nano-ribbon
SPICE	Simulation Program with Integrated Circuit Emphasis
SWCNT	Single Walled Carbon Nanotube
SLGNR	Single Layer Graphene Nano-ribbon
TC-MLGNR	Top Contact Multi-Layer Graphene Nano-ribbon
VLSI	Very Large Scale Integration
zz-GNR	Zigzag Graphene Nano-ribbon

## LIST OF FIGURES

---

S.No.	Figure Details	Page No.
<b>Figure 1.1</b>	Lattice structures of (a) Graphene (b) CNTs (hollow cylinder graphene sheets) (c) SLGNR (patterned graphene sheet) (d) MLGNR (patterned graphite).	2
<b>Figure 1.2</b>	(a) Armchair GNR chirality (b) Zigzag GNR chirality	4
<b>Figure 2.1</b>	Resistance per unit length for MLGNR, SWCNT-bundle and copper interconnects.	9
<b>Figure 2.2</b>	RLC delay ratio w.r.t. copper wire for global interconnects	10
<b>Figure 2.3</b>	Comparison between optical and MLGNR interconnects in terms of delay	12
<b>Figure 3.1</b>	Geometry of MLGNR interconnects	15
<b>Figure 3.2</b>	An equivalent circuit model of SLGNR interconnects.	15
<b>Figure 3.3</b>	Resistance per unit length for (a) TC-MLGNR and (b) SC-MLGNR	19
<b>Figure 4.1</b>	Mean free path as function of temperature	25
<b>Figure 4.2</b>	Resistance of MLGNR and copper interconnects	26
<b>Figure 4.3</b>	Temperature dependent and independent resistance of MLGNR interconnects as a function of length.	27

<b>Figure 4.4</b>	Interconnect line connected with load and a driver	29
<b>Figure 4.5</b>	Temperature dependent and independent delay of MLGNR interconnects as a function of length	29
<b>Figure 4.6</b>	Temperature dependent and independent power dissipation of MLGNR interconnects as a function of length.	31
<b>Figure 4.7</b>	Temperature dependent and independent power delay product (PDP) of MLGNR interconnects as a function of length	32
<b>Figure 4.8</b>	Power spectrum in dB with respect to frequency of MLGNR interconnects at different temperatures	33
<b>Figure 5.1</b>	Capacitively coupled distributed RLC interconnects driven by CMOS inverter	36
<b>Figure 5.2</b>	Temperature dependent crosstalk induced transient response of the victim output for MLGNR interconnects	36
<b>Figure 5.3</b>	Variation in the time duration of output waveform of victim net for the temperature dependent and independent model of MLGNR	37
<b>Figure 5.4</b>	Variation of normalized crosstalk amplitude of frequency components with normalized signal frequency as a function of temperature variations for MLGNR at the far end of victim line	39
<b>Figure 6.1</b>	Temperature-dependent delay of MLGNR and copper at 14nm technology node with 1mm long interconnect	41
<b>Figure 6.2</b>	Temperature dependent power dissipation of MLGNR and copper at 14nm technology node with 1mm long interconnect	42
<b>Figure 6.3</b>	Power delay product (PDP) of MLGNR and copper interconnects as a function temperature	42
<b>Figure 6.4</b>	Power spectrum in dB with respect to frequency of MLGNR and Cu interconnects	43
<b>Figure 6.5</b>	Temperature dependent crosstalk induced transient response of coupled interconnects	44

<b>Figure 6.6</b>	Variation in the time duration of output waveform of victim net of MLGNR and copper at different temperatures from 300K to 500K	45
<b>Figure 6.7</b>	Variation of normalized crosstalk amplitude of frequency components with normalized signal frequency as a function of temperature variations for copper at the far end of victim line.	46

## LIST OF TABLES

---

<b>S.No.</b>	<b>Figure Details</b>	<b>Page No.</b>
<b>Table 4.1</b>	Simulation Parameters from ITRS 2012	25
<b>Table 4.2</b>	Impedance parameters of interconnects, technology = 14nm	28
<b>Table 4.3</b>	Average improvement in delay	30
<b>Table 4.4</b>	Average improvement in power dissipation	31
<b>Table 5.1</b>	Average improved reduction in time duration of transient response at the victim output of temperature dependent model with that of temperature independent model.	38
<b>Table 6.1</b>	Improvement (%) in power bandwidth of MLGNR as compared to Cu	44
<b>Table 6.2</b>	Average improved reduction in time duration of transient response at the victim output of MLGNR with that cooper interconnects.	45

## LIST OF SYMBOLS

---

$\lambda_{eff}$	Effective mean free path of MLGNR
$E_f$	Fermi Energy
$v_f$	Fermi velocity of electrons
$N_{ch}$	Number of conducting channels
n	Number of layers
$C_e$	Electrostatic capacitance
$C_g$	Ground capacitance
$C_q$	Quantum capacitance
$C_c$	Coupling capacitance
$L_k$	Kinetic inductance
$L_m$	Magnetic inductance
$L_s$	Self-inductance
Cu	Copper
$R_c$	Contact resistance
$R_q$	Quantum resistance

$R_s$	Scattering resistance
E	Dielectric constant
$\rho_c$	c-axis resistivity
$\rho_m$	Mass density of graphene
$\rho_0$	Resistivity of copper at 300K
$\mu_0$	Permeability
H	Plank's constant
S	Separation between adjacent interconnects
W	Interconnect width
L	Interconnect length
T	Thickness of interconnects
E	Electron charge
D	Distance between ground and interconnect
$K_b$	Boltzmann's constant
A	Area of cross-section
AsF <sub>5</sub>	Arsenic penta-Fluoride
$\alpha$	Temperature coefficient of resistance
T	Temperature

$\Delta$	Van-der wall gap
$T_c$	Transmission coefficient

**1.1 INTERCONNECTS**

Interconnect is something that provides connection between two elements. In VLSI, interconnect is a narrow sheet of conducting material which provides electrical connection between nodes of an IC. Earlier, aluminium was used as an interconnect material due to its good conductivity and adherence on silicon on silicon dioxide. But with the scaling of technology, aluminium wires showed many disadvantages, such as electromigration. Electromigration in aluminium wires causes resistance of the wires to be increased rapidly. Because of these disadvantages aluminium wires were superseded by copper wires as a VLSI interconnect material. Copper showed many advantages when compared with aluminium, such as high conductivity and resistance to electromigration. Therefore, copper wires became more favourable interconnect material for high performance circuits.

With the continuous scaling of technology, copper interconnect is facing some problems. With the scaling of technology in deep submicron (DSM) region, the resistance of copper interconnects has started to increase due to surface roughness and grain boundary scattering [1]-[9]. The decreased performance of copper in deep submicron (DSM) region is affecting the performance of the high performance circuits. Therefore, research is proceeding to find a better alternative of copper interconnect and the allotropes of carbon such as Carbon nano tubes (CNTs) and Graphene nanoribbons (GNRs) are being recommended as next generation interconnect materials [8-18].

**1.1.1 Why, Allotropes Of Carbon Are Being Recommended As Next Generation Interconnect Materials.**

As the technology is evolving the performance of interconnects in a circuit that was once neglected is now turning out to be major concern for the high performance integrated circuits. It has been realized that with the scaling of technology in deep submicron (DSM) region, the resistance of consistently used copper (Cu) interconnects has started to increase due to surface roughness and grain boundary scattering [1]-[9]. This increase in resistivity of copper interconnects causes degradation in the performance of copper interconnects in terms of signal

delay and power dissipation. Also, with the constant scaling in technology, the feature size of chip keeps decreasing. This causes the spacing between the adjacent interconnect wires to decrease. There is also a significant decrease in the lateral width of interconnect wires as compared to their vertical height. Due to these cases, the coupling capacitance between the wires increases rapidly [19-22]. This increases the problem of crosstalk noise the copper interconnects. Therefore, research is proceeding to find a better alternative of copper interconnects.

The allotropes of carbon such as Carbon nano tubes (CNTs) and Graphene nanoribbons (GNRs) are being recommended as next generation interconnect materials [8-17]. GNRs and CNTs are derived from graphene which can be described as a single layer of carbon atoms packed in the 2-D honeycomb lattice structure. CNT can be obtained by rolling up a graphene sheet as a hollow cylinder and GNR can be obtained by patterning graphene into thin strips, shown in Fig 1.1 [8].

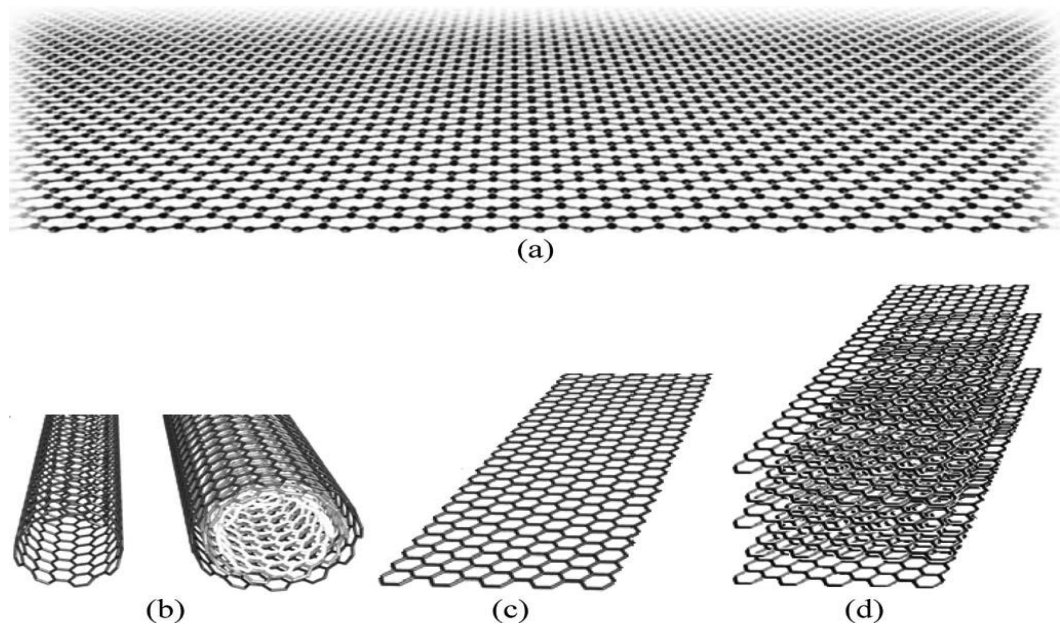


**Figure 1.1:** Lattice structures of (a) graphene, (b) CNTs (hollow cylinder graphene sheets) [left one is SWCNT and right one is MWCNT], (c) SLGNR (patterned graphene sheet), and (d) MLGNR (patterned graphite) [23].

CNT and GNR both display better electrical, thermal, and mechanical properties when compared to copper. Both GNR and CNT have long mean free path (MFP), high current density and high thermal conductivity when compared with Cu [11-18], [24], [25]. Also,

CNTs and GNRs have immunity to electro-migration due its strong atomic carbon-carbon bond. Due to these advantages, GNRs and CNTs are being preferred as future material for system on chips interconnects. However, GNR is easy to control as compared to CNTs in terms of chirality due to its planar geometry. Also the fabrication process of CNT is more complex as compared to GNR [13], [25]. Therefore profound study of GNR's major performance parameter is required to determining its overall performance as the future interconnects material.

## 1.2 GRAPHENE NANO-RIBBON (GNR)

Graphene nano-ribbons (GNRs) have been considered as a potential interconnect material to replace copper interconnects in deep submicron (DSM) technology region. GNR can be obtained by patterning graphene, a single layer of carbon atoms packed in the 2-D honeycomb lattice structure as shown in Fig. 1.1(a), into thin strips [17]. GNRs are been considered as a future material for VLSI interconnects due to its remarkable properties, such as:

### 1.2.1 GNRs Properties [8, 18, 26]

- [1] Long mean free path (MFP)  $\sim [1 \times 10^3 \text{ nm}]$
- [2] High current density  $\sim [5 - 20 \times 10^8 \text{ A/cm}^2]$
- [3] High thermal conductivity  $\sim [3 - 5 \times 10^3 \text{ W/mK}]$
- [4] High mobility of graphene
- [5] Ambipolar in nature i.e., conduction is carried by both electrons and holes.
- [6] High melting point  $\sim [3773\text{K (graphite)}]$

### 1.2.2 Types Of GNRs

A. Depending upon shape of their edges, GNRs can be categorized into two types:

1. Zigzag GNRs (zz-GNRs) – predominately metallic
2. Armchair GNRs (ac-GNRs) – metallic and semiconducting

The structures of both zz-GNRs and ac-GNRs are shown Fig. 1.2. Armchair GNRs can be further sorted into metallic and semiconducting ac-GNRs. If the number of carbon rings along its width is  $3p+2$ , the ac-GNR has metallic properties. If the number of carbon rings along its width is  $3p$  and  $3p+1$ , the ac-GNR has semiconducting properties. Zigzag GNRs are predominately metallic in nature and has less resistance when compared to armchair GNRs, at  $w < 5\text{nm}$  [26], [8]. In VLSI applications only metallic nature interconnects are used [3].

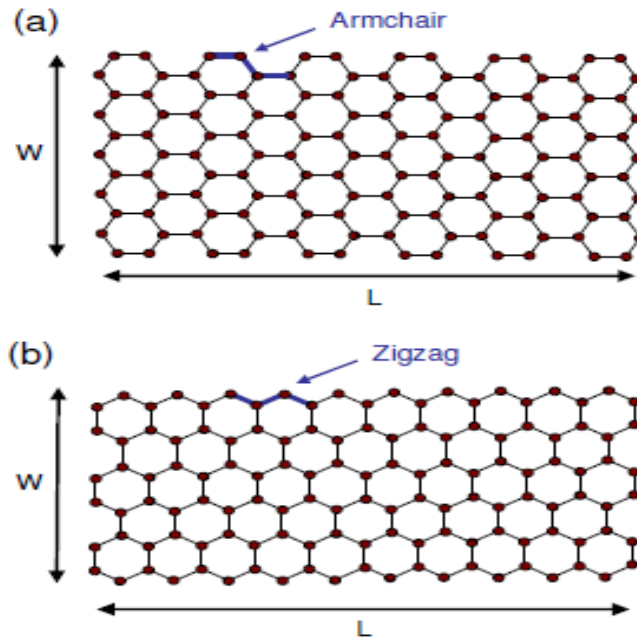


**Figure 1.2:** (a) Armchair GNR chirality, and (b) Zigzag GNR chirality [27].

B. Based upon the connection of surrounding devices, GNRs can be classified as,

1. Top contact GNRs (TC-GNRs)
2. Side contact MLGNR (SC-GNRs)

In the case of TC-GNRs, only top layer is connected with contacts and in the case of SC-MLGNR, all single layer GNRs are physically connected. It has been reported that the SC-MLGNR has better performance when compared to TC-MLGNR [14]. This is due to less equivalent resistance offered by SC-MLGNR as compared to TC-MLGNR.

C. Based upon the number stacked graphene sheets, GNRs can be classified as,

1. Single layer GNRs (SLGNRs)
2. Multilayer GNRs (MLGNRs)

Single/Monolayer GNR (SLGNR) and Multilayer (MLGNR) are shown in Fig. 1.1 (c) and (d). It has been noted that SLGNRs consists a large intrinsic resistance, therefore MLGNR as shown in Fig. 1.1(d), is used as an interconnect [25].

### **1.2.3 Performance Comparison Of GNR With Other Materials**

Both GNR and CNT have long mean free path (MFP), high current density and high thermal conductivity when compared with Cu [11-18], [24], [25]. However, GNR is easy to control as compared to CNTs in terms of chirality due to its planar geometry. Also the fabrication process of CNT is more complex as compared to GNR [13], [25]. But GNRs need to have multiple layers along proper intercalation doping and match the performance of global level copper or SWCNT interconnects.

#### **Advantages of GNRs:**

- a. Easy to control: Due to its planar nature the chirality of GNRs can be easily controlled using high resolution lithography as compared to CNTs.
- b. Easy to fabricate: The fabrication process of CNT is more complex as compared to GNR [13], [25].
- c. Large mean free path (MFP) and high current density as compared to copper [11-18], [24], [25].
- d. Better electrical, thermal, and mechanical properties compared to copper [26].

#### **Issues in GNRs:**

- a. GNRs face a problem of edge scattering which in result reduce its mean free path (MFP). CNTs do not have such problem.
- b. Beyond 22nm technology node, when compared using resistance model, SWCNT bundles turn out to be better than copper and GNR interconnects. All the GNR structures are not better than copper.
- c. Single layer GNR (SLGNR) consists of large mean free path (MFP) and conductivity. But multilayer GNR (MLGNR) experience intersheet electron hopping and has much lower conductivity per layer .[26]

### **1.3 STATEMENT OF THE PROBLEMS**

As the technology scaled down, it is observed that the temperature of interconnects based on conventional material (copper) increases beyond a 45 nm node due to the combined effect of increase in resistivity of metal and current density. Operating temperature of most of the integrated circuit is much greater than room temperature. Thus, there is an essential need to understand the temperature dependent electrical characteristics of GNRs greater than room temperature. It has also been noted that the density of the interconnection in the chip has increased with device scaling and resulted in higher crosstalk, very few researcher till date

have studied the effect of crosstalk in MLGNR. However, no studied has been made to analyze the thermally aware performance analysis of MLGNR, in terms of crosstalk, delay and power.

- **Objectives**

The following are the objectives of the proposed study:

- ✓ Development of temperature dependent circuit parameters of MLGNR based interconnects.
- ✓ Temperature dependent analysis of propagation delay and power dissipation in MLGNR interconnects.
- ✓ Temperature dependent analysis of crosstalk and its frequency spectrum in coupled interconnects of MLGNR.
- ✓ Comparison of temperature dependent delay, power, crosstalk and frequency spectrum analysis of MLGNR interconnects with copper interconnects at 14nm technology nodes.

## **1.4 ORGANIZATION OF THE THESIS**

**Chapter 1** provides a brief introduction of the subject of the proposed work.

**Chapter 2** includes a brief review of the previous work done on the topic of interconnects, beginning from the basics to the advance work done on the topic of GNRs. A brief survey of the previous works done by researcher on interconnect materials are presented. The recent studies on the modelling and performance of GNR based interconnects are also presented.

**Chapter 3** presents the temperature dependent circuit modeling of MLGNR based interconnects. Equivalent single conductor (ESC) model of individual GNR is derived by considering the parasitic elements like resistance, capacitance and inductance.

**Chapter 4** includes the performance and impedance analysis of MLGNR based interconnects. Firstly in the chapter, briefs about the temperature dependent impedance analysis for MLGNR and copper based interconnects are presented. Then the performance analysis of MLGNR of temperature dependent model in terms of propagation and power dissipation at 14nm technology node is shown and compared with temperature independent model.

**Chapter 5** of the thesis shows the temperature dependent crosstalk and its frequency spectrum analysis. This chapter explicates the effect of temperature variations on the crosstalk induced noise voltage and its frequency spectrum between coupled interconnect. The crosstalk

amplitudes for varied frequencies of temperature dependent model are compared with the temperature independent one.

**Chapter 6** presents the comparative study between MLGNR and copper based interconnects. The performance of MLGNR based interconnects in terms of propagation delay, power dissipation, crosstalk noise voltage and its frequency spectrum, is compared with that of conventionally used copper based interconnects for different temperature ranging from 300K to 500K and at different global lengths ranging from 1000 $\mu$ m to 400 $\mu$ m.

**Chapter 7** contains the conclusion and future scope of the thesis.

**2.1 INTRODUCTION**

Due continuous scaling of technology and decrease in device dimensions, the effect of interconnects performance that was previously neglected is becoming crucial for integrated circuits. As the number of connections per area is increasing rapidly, the crosstalk noise due to coupled interconnects is becoming a significant problem. Conventionally used interconnect material copper is facing problems like surface scattering and grain boundary with continues reduction in cross-sectional area of interconnects. Therefore, research is impelling towards finding a substitute for copper. Till now, carbon alloys are coming out be a goof alternative of copper due to their great physical properties [8], [11], [17], [18], [26].

This chapter briefly reports the work of many researchers for finding an alternative of copper interconnects. This chapter also describes work of authors on GNR and possibility of GNR being the next generation interconnects. Section 2.2 shows the work done by different authors over the years on modelling and performance of MLGNR interconnects. A brief conclusion of this chapter is given in section 2.3.

**2.2 LITERATURE REVIEW**

**T. Ragheb and Y. Massoud, 2008[27]** provided a comprehensive resistance model for the graphene nano-ribbon (GNR) interconnects. Utilising recently done experiments and theoretical results, they modelled the effect of stacking of graphene layer in multi-layer GNR (MLGNR). Resistance of GNR is compared with single-wall carbon nanotube (SWCNT) and traditionally used copper interconnects in this paper. The comparison between resistance of SWCNT, Cu and MLGNR for different width of interconnects is shown in Fig. 2.1. From Fig. 2.1 it is observed that MLGNR has lowest resistance as compared to both SWCNT and copper interconnects. The results of the simulations show the superiority in performance of MLGNR over traditionally used copper interconnects at small lengths (<15 nm). Further the paper states that as the feature size is decreasing in VLSI industry, MLGNR interconnects can be used instead of copper interconnects in future. It has been observed in the paper that due to

MLGNR's immunity to electro-migration, less temperature-dependence and ease of fabrication, GNR-based technology can provide great substitute for future interconnects.

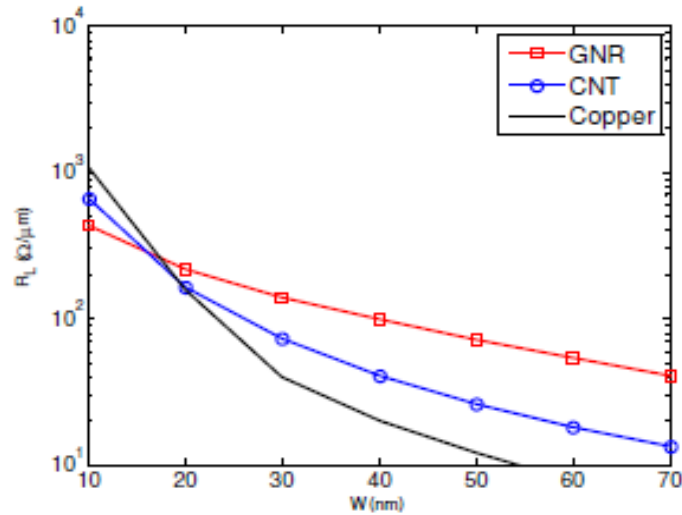


**Figure 2.1:** Resistance per unit length for MLGNR, SWCNT-bundle and copper interconnects [27].

**K. Banerjee *et al.*, 2009[26]** proposed a conductance and delay analysis of GNR interconnect. An observation has been made on the effect edge specularity has on the conductance of GNR interconnects. Comparison is done on the performances of GNR with CNT and copper in the paper. The results state that GNRs have some advantages in terms of fabrication as compared to CNTs. But some definite technology improvement must need to be attained in case of GNRs to make them better than its counterparts i.e., copper and CNTs. A delay comparison is done between AsF5 doped MLGNR and SWCNT interconnects as shown in Fig. 2.2. The Fig. 2.2 shows that, as compared to SWCNT, SLGNR and MLGNR with rough edges, the AsF5 doped MLGNR with perfect edges has lower delay ratio. The result revealed that for MLGNR to be comparable or to be better than copper and carbon nanotube, zz-MLGNR needs to have very specular edges ( $p > 0.8$ ) and should have appropriate intercalation doping at both local and global lengths. The paper should that intercalation doped zz-MLGNR can be better in performance as compared to tungsten (W), (even for  $p=0$ ) at local lengths, suggesting possible use of zz-MLGNR as local interconnects in some cases.

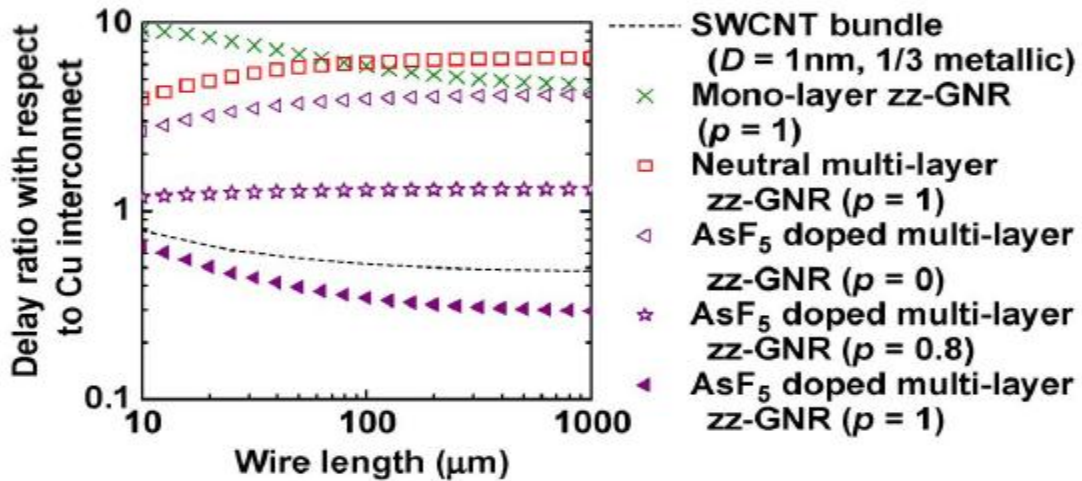


Figure 2.2 RLC delay ratio w.r.t. copper wire for global interconnects [26]

Naeemi *et al.*, 2012 [25] explained a physical model for the effective resistance of multi-layer graphene nano-ribbon (MLGNR). They took c-axis resistivity of MLGNR into consideration for the explanation of this model. They found that a saturation point is attained for effective resistance when numbers of layers are increased. The optimal number of layers are analyzed to minimize the propagation delay and energy-delay product of MLGNR interconnects. It is observed that interconnect length, interlayer resistance and the kind of contact that is used, all of these effects the optimal number of layers. It is shown that, when the GNR edges are smooth and if minimum-sized drivers are used, then the delay of MLGNR is lower than that of copper interconnects. If the GNR has rough edges, then the MLGNR based interconnects has lower propagation delay as compared to copper interconnects. They established that the energy delay product (EDP) of MLGNR interconnects is low as compared to copper based interconnects, when edges are smooth and fermi energy ( $E_f$ ) = 0.2 eV.

A.G. Chiariello, A. Maffucci, 2012[30] gave the performance analysis of global-level on-chip interconnects. The paper presented a simple circuit equivalent model for both carbon and graphene nano-ribbon. The circuit modelling of carbon nanotube and graphene nano-ribbon interconnects, takes size and the thermal effects into consideration. The change in number of conducting channel with the temperature is calculated, while assuming the mean free path of GNR constant with temperature. It was revealed that as compared to copper and SWCNT based interconnects, GNR and MWCNT based interconnects were less sensitive to temperature change.

**A. Maffucci and G. Miano, 2013[33]** presented a model for the signal propagation in graphene nano-ribbon (GNR) interconnects. The behaviour of number of conducting channels are analysed for armchair and zigzag GNRs with the variation of width. In this paper both kinetic inductance and quantum capacitance are expressed in terms of number of conducting channels. Using the semi classical Boltzmann transport theory, the number of productive conducting channels was estimated.

**V. Kumar *et al.*, 2013[28]** made an assessment analytical models of multi-layer GNR (MLGNR) with top contacts that were developed earlier. A comparison is made between multi-conductor transmission line (MTL) models and the simplified equivalent distributed RC model for GNR. The MTL models shows the distributed of current among different layers along the interconnect length. They found that frequency response of GNR interconnects can be precisely predicted using multi-conductor transmission line (MTL) models. For minimizing the propagation delay and energy-delay product (EDP), the optimal number of GNR layers was derived using the distributed RC models. Further in the paper, it was found that for small interconnects length, multi-layer GNR (MLGNR) with perfect edges is better in performance compared to Cu interconnects.

**W. S. Zaho and W. Y. Yin, 2014[24]** theoretically examined the transmission performance of MLGNR based interconnects for both top and side contact cases, using their ESC model. They noted that the number of conducting channels ( $N_{ch}$ ) of a metallic MLGNR interconnects depends linearly upon width and Fermi energy ( $E_F$ ). Further they developed equivalent inductance and capacitance equations for the ESC model. It was established that for the smaller lengths of interconnect, side contact MLGNR has less equivalent resistance as compared to top contact MLGNR. They proved that at semi-global level, the performance of MLGNR based interconnects is better when compared to copper based interconnects. The performance advantages of MLGNR based interconnects over copper based interconnects can be maintained even after the maximum crosstalk effect is considered upon MLGNR interconnects. According to them Fermi energy and edge roughness are two crucial factors that affects the performance of MLGNR based interconnects.

**A. K. Nishad and R. Sharma, 2014[14]** presented the analytical models for both top and side contact multilayer GNR (SC-MLGNR). They stated that when compared, side contact MLGNR (SC-GNR) is better in performance than the top contact MLGNR (TC-MLGNR), but the fabrication of side contact MLGNR is much more complex. They provide an optimized

design of top contact MLGNR, so that its performance is better than copper. The performance of the optimized design matches the performance of the side contact MLGNR. They also did a comparison between optical interconnects and top contact MLGNR interconnects and it was found that top contact MLGNR's performance surpasses the performance of optical interconnects in terms of propagation delay as shown in Fig. 2.3. From the Fig. 2.3, it can be clearly noted that for the interconnect lengths less than 500 $\mu\text{m}$  MLGNR is better in performance as compared to optical interconnects in terms of propagation delay.

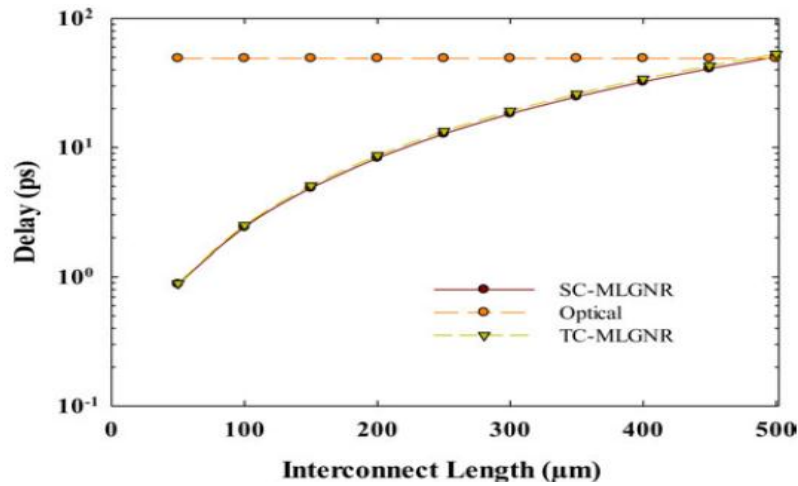


**Figure 2.3** Comparison between optical and MLGNR interconnects in terms of delay [14].

**B.K. Kaushik et al., 2015[15]** examined the effect of doping on the performance of MLGNR interconnects and noticed that the conductivity of doped MLGNR is high as compared to a neutral MLGNR. Comparison is also done between the performance of doped MLGNR and copper interconnects in terms of delay, power dissipation and bandwidth using ESC model. It was found that, for the similar dimensions, the power dissipation and delay of doped MLGNR was smaller by 86.13% and 43.72%, respectively, when compared to copper interconnects. They noticed that, at the intermediate and global interconnect lengths the doped MLGNR has four times higher bandwidth when compared to copper interconnects due to its smaller parasitics. Comparison is done between the performance of MLGNR with different edge roughness and copper interconnects. They witnessed a significant change in the performance of MLGNR interconnects with higher edge roughness.

**M. K. Rai et al., (2016) [8]** studied the effect that interlayer resistance has on the performance of MLGNR based interconnects due to its contact resistance and c-axis resistivity. They also noticed the effect that Fermi energy have on the performance of MLGNR interconnects. For their study they included the capacitance and inductive coupling between the adjacent layers

of MLGNR. They compared the performance of MLGNR interconnects with that of copper based interconnects on the basis of propagation delay, power dissipation and power delay product (PDP), at 22nm technology node. It was noticed that MLGNR is much better in performance when compared to copper interconnects for intermediate to global interconnect lengths (300 $\mu$ m to 1000 $\mu$ m). They also examined that the performance gap between MLGNR with and without interlayer resistance decreases with increase in fermi energy.

**M.K. Rai et al., 2014[19]** addressed the impact of temperature on the crosstalk induced noise voltage and its frequency spectrum at the far end of victim line, for SWCNT bundle. For their analysis, they took capacitive coupling between adjacent SWCNT interconnect lines. At 22nm technology node, they compared the results of similar analysis done on copper interconnects with that of MLGNR based interconnects. It was found that crosstalk noise voltage levels are quite low for CNT as compared to copper based interconnects, at different temperature ranging from 300K to 500K. It was also noticed that with increase in temperature from 300K to 500K, the CNT based interconnects filter more noise frequency components when compared with copper based interconnects.

### **2.3 CONCLUSION**

It is observed that the resistance of MLGNR is much less than the copper based interconnects. Due to the less resistance offered by MLGNR, the performance in terms of propagation delay of MLGNR is better than the conventionally used copper interconnects. Various models of GNR are reviewed to analyse the performance of GNR as future VLSI interconnect. Performance comparison of SLGNR, MLGNR and AsF5 doped MLGNR is analysed and AsF5 doped MLGNR gave the best results for different interconnect lengths. Side contact and top contact MLGNR interconnects are thoroughly analysed and compared. This literature survey raises many research gaps in the previous studies. There is no major work done on the effect that temperature has on the performance of GNR based interconnects. Also, there is need of thorough study on the temperature dependence of crosstalk noise levels and its frequency spectrum, to consider it as a next generation interconnect material.

**3.1 INTRODUCTION**

As the technology is evolving the performance of interconnects in a circuit that was once neglected is now turning out to be major concern for the Engineers. It has been realized that with the scaling of technology the consistently used interconnect material, Cu is confronting problems like increase in temperature and increase in propagation delay due to quick rise in its resistivity and current density. Excessive temperature increase can cause heating and damaging of device. Therefore thermal issues are becoming major factor while choosing an interconnect material for designing high performance integrated circuits. Integrated circuits with high performance are sensitive to temperature variation, therefore a better alternative of copper interconnect is essential. Carbon allotropes such as Carbon nano (CNT) tube and Graphene nanoribbon (GNR) are being recommended as next generation interconnect materials. Multi-layer graphene nano-ribbon (MLGNR) is considered to be future interconnect material because it is easy to control as compared to CNTs in terms of chirality due to its planar geometry. This chapter describes temperature dependent impedance parameters of MLGNR and Cu interconnect at 14nm technology node. Two different resistance models of MLGNR are given, depending upon the types of contact used (side or top contact).

**3.2 TEMPERATURE DEPENDENT AND INDEPENDENT MODELLING OF MLGNR**

This section presents an analytical model of MLGNR based on the geometry. The MLGNR is viewed as the stack of SLGNRs as shown in Fig. 3.1. Therefore, it can be studied based on the equivalent single conductor (ESC) model of MLGNR [15]. The ESC model of MLGNR is a combination of ESC models of parallel SLGNRs. Initially, the simple ESC model of individual GNR is derived by considering the parasitic elements like resistance, capacitance and inductance as shown in Fig. 3.2. Later, these equivalent circuit models are combined to build up the final ESC distributed RLC model of MLGNR. The improved circuit parameters (R, L and C) of MLGNR under the evidence of temperature are obtained from the expressions available in literature [12], [24], [31],[31].

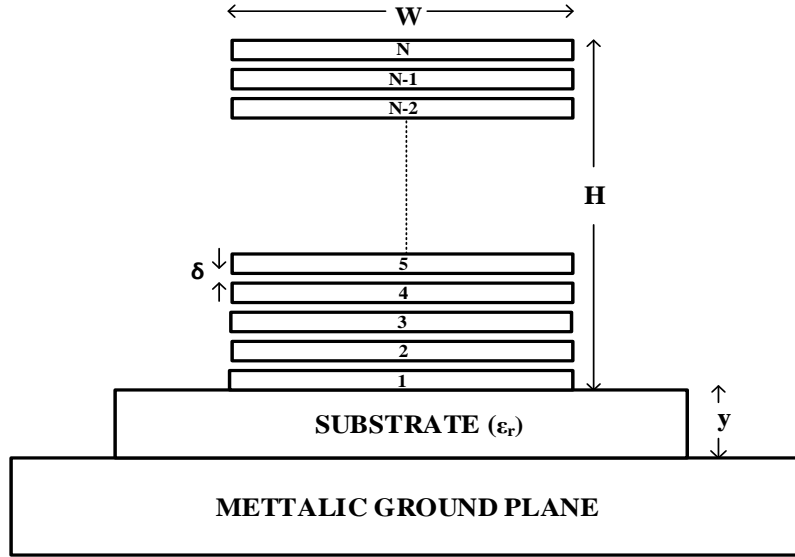


**Figure 3.1:** Geometry of MLGNR interconnects [35].

Where  $\delta$  is known as van-der waal gap and has a value of 0.34nm.  $W$  is width of the interconnect material and  $H$  is the thickness of the material.  $N$  is the total number of layers in MLGNR and can be found using Eq. (3.1) [22].

$$n = 1 + \text{round} \left( \frac{t}{\delta} \right) \quad (3.1)$$

Where  $t$  is thickness and  $\delta$  is van-der waal gap of MLGNR.

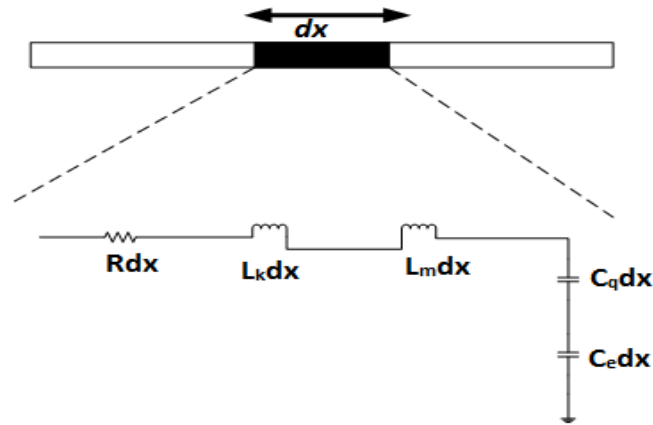


**Figure 3.2:** An equivalent circuit model of SLGNR interconnects [35].

### 3.2.1 Temperature Dependent Modeling Of MLGNR

In order to model MLGNR interconnects, we need to consider the parameters that depends on temperature. Also there is a need to investigate the types and source of scattering that occurs due to temperature and that impact the parameters of MLGNR. Mean free path and channel length of MLGNR are two parameters that are dependent upon temperature variations.

Mean free path of MLGNR: Temperature dependent effective mean free path can be calculated by Eq. (3.2) [32],[34],[19].

$$\lambda_{eff}(T) = \left[ \frac{1}{\lambda^{AC}} + \frac{1}{\lambda_{abs}^{op}} + \frac{1}{\lambda_{emm}^{op}} \right]^{-1} \quad 3.2$$

Where,  $\lambda^{AC}$  is due to acoustic scattering,  $\lambda_{abs}^{op}$  and  $\lambda_{emm}^{op}$  are due to scattering by optical absorption and emission and are expressed as

$$\lambda^{AC} = 4 \frac{\rho_m \left( \frac{h}{2\pi} v_f v_s \right)^2}{\sqrt{\pi N_s} D_{AC}^2 K_B T} \quad 3.3$$

Where,  $\rho_m = 7.6 \times 10^{-7} \text{ kg/m}^2$  is the mass density of graphene,  $v_s = 20 \text{ km/s}$  is the speed of acoustic phonons,  $v_f = 8 \times 10^5 \text{ m/s}$  is Fermi velocity of electronics,  $D_{AC} = 8\text{eV}$  is the acoustic deformation potential and  $N_s = 4 \times 10^{16} /\text{m}^2$  is the concentration of 2-D electron gas in graphene.

Mean free path due to scattering by optical absorption and emission and are expressed as

$$\lambda_{abs}^{op} = \frac{\rho_m \frac{h}{2\pi} w_{op} v_f^2}{\sqrt{\pi N_s} D_{op}^2 N_{op,abs} \left( 1 + \frac{w_{op}}{v_f \sqrt{\pi N_s}} \right)} \quad 3.4$$

$$\lambda_{emm}^{op} = \frac{\rho_m \frac{h}{2\pi} w_{op} v_f^2}{\sqrt{\pi N_s} D_{op}^2 N_{op,emm} \left( 1 - \frac{w_{op}}{v_f \sqrt{\pi N_s}} \right)} \quad 3.5$$

Where,  $\frac{h}{2\pi} w_{op}$  is the optical phonon energy ( $\sim 160\text{meV}$ ) and  $N_{op}$  is the optical phonon number, and can be calculated as,

$$N_{op} = \frac{1}{\frac{\frac{h}{2\pi} w_{op}}{K_B T} - 1} \quad 3.6$$

- Conducting channels: The number of conducting channels ( $N_{ch}$ ) of an MLGNR depends upon temperature, geometry and material and can be calculated by Eq. (3.7) [36]-[37], given by

$$N_{ch}(T) = \sum_{i=0}^{n_c} (1 + e^{\frac{E_i - E_f}{k_b T}})^{-1} + \sum_{i=0}^{n_v} (1 + e^{\frac{E_i + E_f}{k_b T}})^{-1} \quad 3.7$$

where,  $n_c$  is the number of conduction sub-bands and can be calculated as  $n_c = \frac{2w}{\sqrt{3}a}$ ,  $a = \sqrt{3}b$ , where  $b$  is inter atomic distance [33] and  $n_v$  is the number of valence sub-bands [33].  $E_i$  is the lowest (highest) energy of the  $i^{\text{th}}$ -conduction(valence) sub-band and is given by Eq.(3) [10,17],

$$E_i = \frac{\hbar v_F}{2w} \left( \frac{1}{2} + |i| \right) \quad 3.8$$

,  $i \neq 0$

Here, Fermi energy ( $E_f$ ) of 0.2eV is assumed for GNR [24].

### A. Resistance Modeling

The resistance of MLGNR interconnects can be divided into three components:

- a) The imperfect contact resistance ( $R_c$ )
- b) The quantum resistance ( $R_q$ )
- c) The scattering resistance ( $R_s$ )

#### Contact Resistance ( $R_c$ ):

Contact resistance ( $R_c$ ) of MLGNR occurs due to imperfect contact condition between MLGNR and other materials, therefore it is very process dependent [20]. The  $R_c$  of MLGNR can be calculated by Eq. [12],

$$R_c = \frac{h}{2e^2 N_{ch}(T) T_c} \quad 3.9$$

Here,  $N_{ch}$  is number of conduction channels given in Eq. 3.7,  $h$  is known as planck's constant,  $e$  is the charge of the electron and has a value of  $1.602 \times 10^{-19}$  coulombs (C). Also,  $n$  is number of layers of MLGNR, given by Eq. 3.1 and  $T_c$  is a dimension less factor, known as

transmission coefficient with value less than unity [19]. For the correct calculations, the contact resistance ( $R_c$ ) is assumed to be in the range of 1 k $\Omega$  to 20 k $\Omega$  [15].

### **Quantum Resistance ( $R_q$ ):**

Quantum resistance ( $R_q$ ) is length dependent for longer MLGNR lengths ( $l > \lambda_{GNR}$ ) and for lengths less than MFP ( $l < \lambda_{GNR}$ ) there is a ballistic electron transport within the nano ribbon [18]. Fundamental quantum resistance occurs due to quantum confinement of carriers across the interconnect width. The quantum resistance of single layer graphene nano-ribbon can be calculated from Eq. 3.10

$$R_q = \frac{h}{2e^2 N_{ch}(T)} \quad 3.10$$

### **Scattering Resistance( $R_s$ ):**

The scattering resistance occurs when the interconnect length is more than the mean free path ( $l > \lambda_{eff}(T)$ ). Scattering resistance occurs due to defects, static impurity scattering and line edge roughness scattering [9], [31], [38]. Low bias regime is considered for this analysis because GNR shows perfect ohmic behaviour in low bias and is suitable for VLSI interconnect application. Whereas, at high bias, electric field is very high which causes current to saturate and GNR does not show ohmic behaviour [40].

The temperature dependent scattering resistance ( $R_s$ ) of single-layer GNR (SLGNR) interconnects per unit length can be calculated with Eq. 3.11 [12].

$$R_s = \frac{h}{2e^2} \frac{1}{N_{ch}(T) \cdot \lambda_{eff}(T)} = \frac{12.9}{(N_{ch}(T) \cdot \lambda_{eff}(T))} k\Omega \quad 3.11$$

As shown in Eq. 3.11, scattering resistance of an interconnect line depends upon its number of conducting channels and mean free path, given in Eq. 3.7 and Eq. 3.2.

Determined by the type of contact, MLGNR can be further categorised as top contact (TC-MLGNR) and side contact (SC-MLGNR) with the connection of surrounding devices as shown by Fig. 3.3 [14].

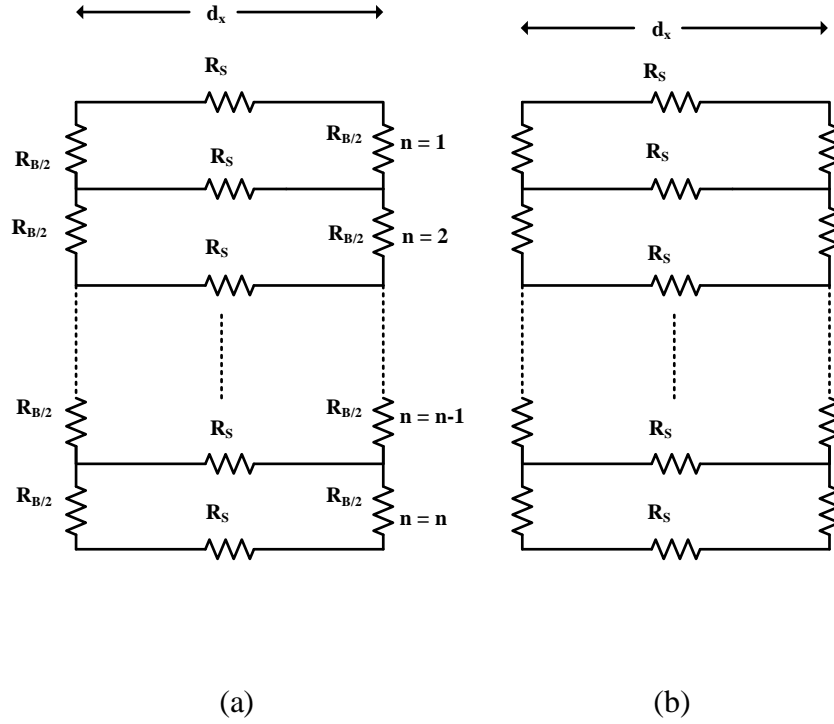


**Figure 3.3:** Resistance per unit length for (a) TC-MLGNR and (b) SC-MLGNR.

Thus, the equivalent low bias resistance of MLGNR varies depending upon the type of contact (i.e. TC-MLGNR or SC-MLGNR).

Firstly, in the case of TC-MLGNR, only top layer is connected with contacts. Therefore, an extra interlayer resistance ( $R_B$ ) comes into the picture with addition to scattering resistance [14]. The equivalent resistance per unit length of TC-MLGNR is given by Eq. 3.12,

$$R_n = \left( \frac{1}{R_S} + \frac{1}{R_{n-1}} \right)^{-1} \quad 3.12$$

Here,  $R_S$  is the scattering resistance and  $R_B$  is the interlayer resistance which can be calculated by Eq. 3.13,

$$R_B = \left( \frac{\rho_c \delta}{\Delta x \cdot w} \right) \quad 3.13$$

Here,  $w$  is the width of interconnect,  $dx$  is the differential element along the interconnect length and  $\rho_c$  is the c-axis resistivity [40].

Secondly, in the case of SC-MLGNR, all single layer GNRs are physically connected. Therefore, for lengths longer than mean free path ( $l > \lambda_{GNR}$ ), the temperature dependent equivalent resistance of SC-MLGNR can be calculated by Eq. 3.14 [12, 14, 24],

$$R_{SC-SLGNR} = \frac{12.9}{N_{ch}(T)} \left(1 + \frac{l}{\lambda_{eff}(T)}\right) \quad 3.14$$

Where,  $l$  is length of interconnect.

It has been reported that the SC-MLGNR has better performance when compared to TC-MLGNR [14]. This is due to less equivalent resistance offered by SC-MLGNR as compared to TC-MLGNR. Lower resistance of SC-MLGNR can give desirable result of decreasing interconnect performance in terms of propagation delay, power dissipation, crosstalk and frequency analysis. Therefore, in this study we assumed MLGNR to be SC-MLGNR.

## B. Inductance Modeling

For GNR, there are two inductances i.e. kinetic inductance ( $L_k$ ) and magnetic inductance ( $L_m$ ) that need to be considered [6, 14, 30]. The kinetic inductance ( $L_k$ ) is the kinetic energy stored in each conducting channel of the GNR. The magnetic inductance ( $L_m$ ) seize the impact of the voltage induced by magnetic fields produced by time varying currents which is outlined in Ampere's Faraday's laws and dependent on the complete current loop. Kinetic ( $L_k$ ) and magnetic ( $L_m$ ) inductances per unit length of MLGNR can be calculated by Eq.3.15 and Eq. 3.16.

$$L_k = \frac{h}{4e^2 v_f n N_{ch}(T)} \quad 3.15$$

$$L_m = \frac{\mu_0 y}{w} \quad 3.16$$

Where  $y$  is the height above the ground plane of MLGNR, shown in Fig. 3.1 and  $\mu_0$  is permeability of free space.

The total inductance of SLGNR interconnect is given by Eq.(3.19),

$$L_{SLGNR} = L_m + L_k \quad 3.17$$

### C. Capacitance Modeling

The capacitance of GNR have two components i.e. quantum capacitance ( $C_q$ ) and electrostatic capacitance ( $C_e$ ) of MLGNR are given by Eq. 3.18 and Eq. 3.19,

$$C_q = \frac{4e^2 n N_{ch}}{h v_f} \quad 3.18$$

$$C_e = \varepsilon. M \left[ \tanh \left( \frac{\pi W}{4d} \right) \right] \quad 3.19$$

Conformal mapping method is used for the calculation of electrostatic capacitance ( $C_e$ ) with width 'w', placed at a distance (y) above the ground plane [16].

The total capacitance of SLGNR interconnect is given by Eq.(3.20),

$$C_{SLGNR} = \frac{C_e \cdot C_q}{C_e + C_q} \quad 3.20$$

To get equivalent capacitance of side contact MLGNR, we need to multiply the equivalent capacitance of SLGNR by the number of grapheme sheets (n) as given in Eq.(3.21).

$$C_{MLGNR} = n. C_{SLGNR} \quad 3.21$$

For equivalent inductance the magnetic inductance ' $L_m$ ' is neglected. This is due to fact that the kinetic inductance is always much larger than the magnetic inductance [24]. Therefore, the equivalent inductance of MLGNR is given as,

$$L_{MLGNR} = \frac{L_{SLGNR}}{n} \approx \frac{h}{4. e^2. v_f. n. N_{ch}(T)} \quad 3.22$$

Similarly, equivalent resistance of MLGNR is given by Eq.3.23

$$R_{SC-MLGNR} = \frac{12.9}{n. N_{ch}(T)} \left( 1 + \frac{l}{\lambda_{eff}(T)} \right) \quad 3.23$$

### 3.3 RLC MODELING FOR COPPER INTERCONNECTS

The performance of copper interconnects due to temperature variation can be estimated through its temperature-dependent resistance, given by Eq. (3.24) [7], [41],

$$R(T) = R_0(1 + \alpha(T - T_0)) \quad 3.24$$

Here,  $\alpha = 0.0039 K^{-1}$  is a temperature coefficient at room temperature [19] and  $R_0$  is resistance of copper at room temperature, given as

$$R_0 = \rho_0 \left( \frac{l}{A} \right) \quad 3.25$$

Here,  $\rho_0$  is the resistivity of copper at room temperature [41]

It can be observed by Eq. 3.23 and 3.24, that the effective low bias resistances of both MLG NR and Cu interconnect are function of temperature.

Other circuit parameters of copper interconnect are self-inductance, ground capacitance and coupling capacitance [41-43].

Self-inductance ( $L_s$ ) of Cu interconnects is given by Eq. 3.26,

$$L_s = \frac{\mu_0 l}{2\pi} \left[ \ln \frac{2l}{w+t} + 0.5 + \frac{0.22(w+t)}{l} \right] \quad 3.26$$

Where  $w$  is width,  $t$  is the thickness of interconnect,  $l$  is length and  $\mu_0$  is permeability of free space.

Ground capacitance ( $C_g$ ) of Cu interconnects is given by Eq. 3.27,

$$C_g = \varepsilon \left[ \frac{w}{d} + 2.22 \left( \frac{s}{s+0.7d} \right)^{3.19} + 1.17 \left( \frac{s}{s+1.15d} \right)^{0.76} \left( \frac{s}{t+4.53d} \right)^{0.12} \right] \quad 3.27$$

Coupling capacitance ( $C_c$ ) of Cu interconnects is given by Eq. 3.28 [19],

$$C_c = \varepsilon \left[ 1.14 \frac{t}{s} \left( \frac{d}{d+2.06s} \right)^{0.09} + 0.74 \left( \frac{w}{w+1.59s} \right)^{1.14} + 1.16 \left( \frac{w}{w+1.87s} \right)^{0.16} \left( \frac{d}{d+0.98s} \right)^{1.18} \right] \quad 3.28,$$

Here,  $d$  is the height above ground,  $s$  is separation between adjacent interconnects and  $\epsilon$  is the dielectric constant.

### **3.4 CONCLUSION**

This chapter introduces temperature dependent modeling of MLGNR interconnects by using an equivalent single conductor (ESC) model. Two distinct resistance models of MLGNR are presented depending upon the type of contact i.e. side or top contact. It is observed that SC-MLGNR has less equivalent resistance as compared to TC-MLGNR. Therefore SC-MLGNR is considered for further analysis. The effect of different types of scattering is remembered while modeling thermally aware mean free path (MFP). RLC modeling of Copper interconnects is also introduced.

**4.1 INTRODUCTION**

It has been realized that with the scaling of technology in deep submicron (DSM) region, the resistance of consistently used copper (Cu) interconnects has started to increase due to surface roughness and grain boundary scattering [1]-[8]. The resistance, inductance and capacitance play an important role in determining the performance of interconnects in terms of propagation delay, power dissipation, power delay product (PDP) and frequency spectrum analysis. Due to better R, L and C values of MLGNR as compared to conventionally used Cu, MLGNR is proposed as futures interconnect material by many researchers.

This chapter presents temperature dependent impedance for MLGNR and Cu interconnects at 14nm technology node. The values of resistance, capacitance and inductance are calculated at distinct global lengths of interconnect varying from 1000 $\mu$ m to 400 $\mu$ m. Resistance, capacitance and inductance are also calculated at different temperatures ranging from 300K to 500K. Variation in their values, with variation in temperature are evaluated. It is noted that compared to inductance and capacitance, resistance value of MLGNR and copper interconnects is highly temperature dependent. Also, the impedance parameters of MLGNR are lesser in value as compared to copper based interconnects. Temperature independent impedance parameters of MLGNR are also analysed.

This chapter further present's temperature dependent performance analysis for MLGNR interconnects at 14nm technology node. Here, the performance of interconnects in terms of delay, power dissipation and power delay product (PDP) and power spectrum under the evidence of temperature is studied. Moreover, temperature independent performance analysis of MLGNR based interconnects is done and compared with the temperature dependent one. It is seen that, there is a significant difference in the performance of temperature dependent and conventionally used temperature independent models of MLGNR based interconnects. Temperature dependent model gives better results as compared to conventionally used temperature independent model.

## 4.2 IMPEDANCE ANALYSIS

This section presents the temperature dependent impedance analysis for MLGNR and copper interconnects at 14 nm technology node. The physical parameters of MLGNR and Cu are taken from ITRS -2012 [44], as demonstrated in Table 4.1 and the circuit models presented in chapter 3 are used for the impedance analysis of MLGNR and copper interconnects. In this study the effect of edge roughness has on MLGNR is ignored because edge roughness can deteriorate the performance of MLGNR as stated by X. Chuan *et al.* [17].

**Table 4.1:** Simulation Parameters from ITRS 2012 [44].

Technology Node 14nm	Local	Semi-Global	Global
Width of Global interconnect ( $w$ )	12nm	12nm	18nm
Separation between adjacent interconnect nets ( $s$ )	12nm	12nm	18nm
Thickness of interconnect ( $t$ )	24nm	24nm	42nm
$\epsilon_r$	4.2	3.604	3.64
$\rho_{cu}(\mu\Omega.cm)$	9.74	9.74	7.02

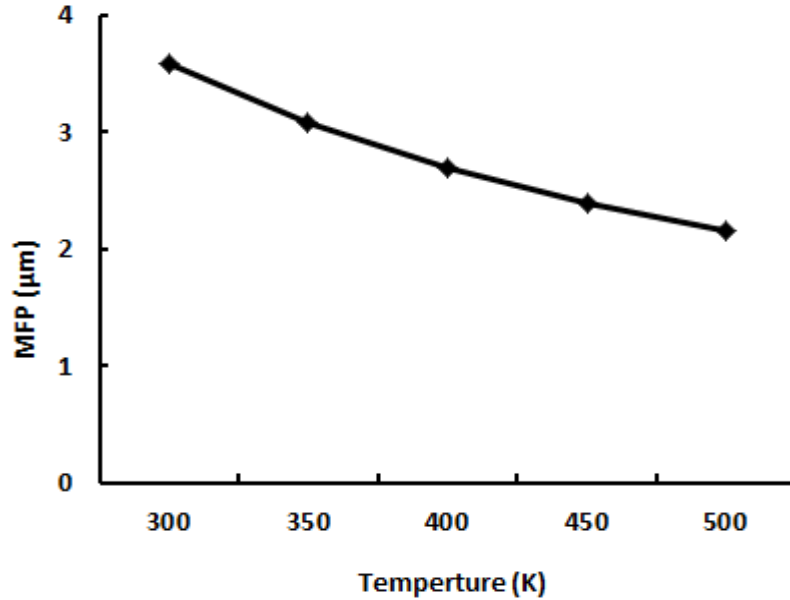


**Figure 4.1:** Mean free path as function of temperature.

Mean free path (MFP) and number of conducting channels ( $N_{ch}$ ) are both temperature dependent parameters as can be seen from Eq. 3.2 and Eq. 3.7. In this analysis, it is noted from

Eqs.(2) and (3) that the impact of temperature variations on number of conducting channels are negligible and result in a negligible effect on capacitance and inductance. Therefore, the capacitance and inductance are approximately constant with temperature variation, ranging from 300K to 500K.

However, mean free path (MFP) vary significantly with temperature as shown in Fig. 4.1. It can be observed that the value of MFP decreases with the increase in temperature. This is because of the fact that scattering increases as temperature rises above the room temperature.

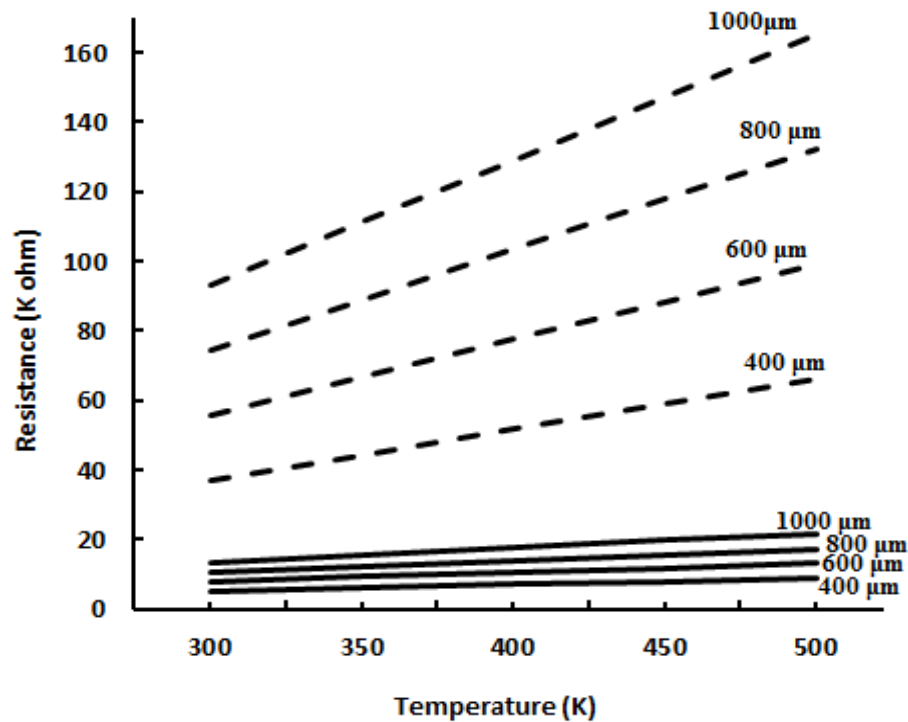


**Figure 4.2:** Resistance of MLGNR and copper interconnects as a function of temperature at different interconnect lengths. The solid lines represent MLGNR and the dash lines represent copper.

From Eq. 3.23, it can be noted that resistance of MLGNR depends upon temperature dependent mean free path of electrons. Fig. 4.2 shows the variation in low bias resistance of MLGNR and copper interconnects at different lengths ranging from 1000μm to 400μm, with the rise in temperature from 300K to 500K.

It is noted that the resistance for both MLGNR and copper increases with rise in temperature at different interconnect lengths, as shown in Fig. 4.2. It can also be seen from Fig. 4.2 that, with rise in temperature from 300K to 500 K, the resistance of MLGNR is very low as

compared to copper interconnect at different interconnect lengths ranging from 400 $\mu\text{m}$  to 1000 $\mu\text{m}$ . This is because of weak variation of temperature-dependent scattering in GNR compared to copper. It can also be noted from Fig. 4.2, that the longer interconnects are more affected by temperature as compared to smaller interconnects.

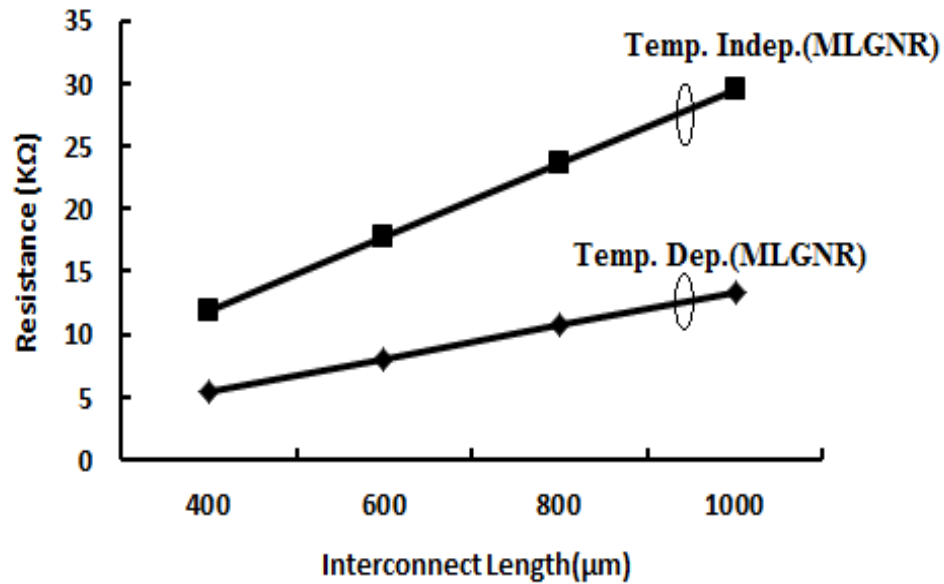


**Figure 4.3:** Temperature dependent and independent resistance of MLGNR interconnects as a function of length.

Further, Fig. 4.3 demonstrates the difference in the resistance of temperature dependent model and temperature independent model of MLGNR. For temperature independent model the mean free path (MFP) is considered to be 1 $\mu\text{m}$  as recommended in [17-18, 32]. In Fig.4.3, resistance calculated from temperature dependent and independent model are plotted at different interconnect length ranging from 400 $\mu\text{m}$  to 1000 $\mu\text{m}$ . It can be observed that the resistance value of temperature dependent model of MLGNR is less than that of temperature independent model. Therefore, it is important to take the temperature dependent model of MLGNR into consideration while doing study on MLGNR as a future interconnect material.

**Table 4.2:** Impedance parameters of interconnects, technology = 14nm.

Length of interconnect		Resistance ( $k \Omega$ )		Capacitance (fF)	Inductance (nH)
		Temperature-dependent resistance at temperature 300 K ( $k \Omega$ )	Temperature-independent resistance ( $k \Omega$ )		
$l=1000\mu\text{m}$	Copper	92.857	92.857	42.231	2.1829
	MLGNR	13.3402	29.507	38.367	29.829
$l=800\mu\text{m}$	Copper	74.286	74.286	33.785	1.7106
	MLGNR	10.6817	23.605	30.694	23.863
$l=600\mu\text{m}$	Copper	55.714	55.714	25.338	1.2484
	MLGNR	8.0232	17.704	23.020	17.897
$l=400\mu\text{m}$	Copper	37.143	37.143	16.892	7.9984
	MLGNR	5.3647	11.803	15.347	11.932

It can be seen from Table 4.2, that the capacitance and inductance increases with the increase in length of interconnect. Also, the capacitance of MLGNR is lower as compared to copper interconnects.

### 4.3 PERFORMANCE ANALYSIS

Delay and power dissipation of interconnects are affected by its circuit parameters [45], [46]. As the resistance of interconnects changes with its temperature due to variation of electron mean free path with temperature. Thus, it is an important need to study the performance of interconnects under the evidence of temperature. In this study, a distributive *RLC* circuit of an equivalent interconnect with CMOS as a driver has been considered, as shown in Fig. 4.4.

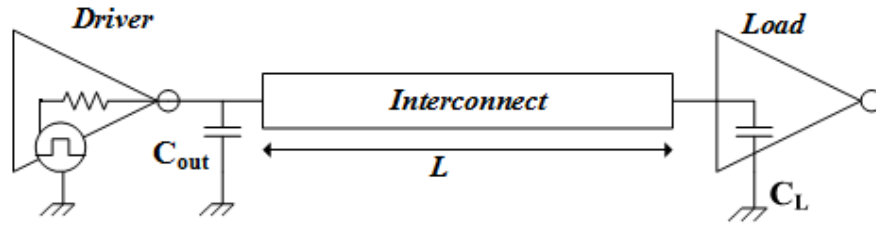


**Figure 4.4:** Interconnect line connected with load and a driver.

To perform simulation, 14nm technology node is taken with a clock speed of 0.1 GHz,  $V_{dd} = 0.8V$  and terminated with capacitive load of 1fF [4]. All these simulation parameters are kept same for both copper and MLGNR. This simulation setup is used with optimum number of repeaters. In this section, the comparative performance analysis in terms of 90% propagation delay, power dissipation and power delay product (PDP) is investigated by using temperature-dependent and independent models of MLGNR.

### 4.3.1 Delay Analysis

90% propagation delay of 1mm long interconnect of MLGNR, as a function of temperature varying from 300K to 500 K at 14nm technology node, has been extracted by simulation results.

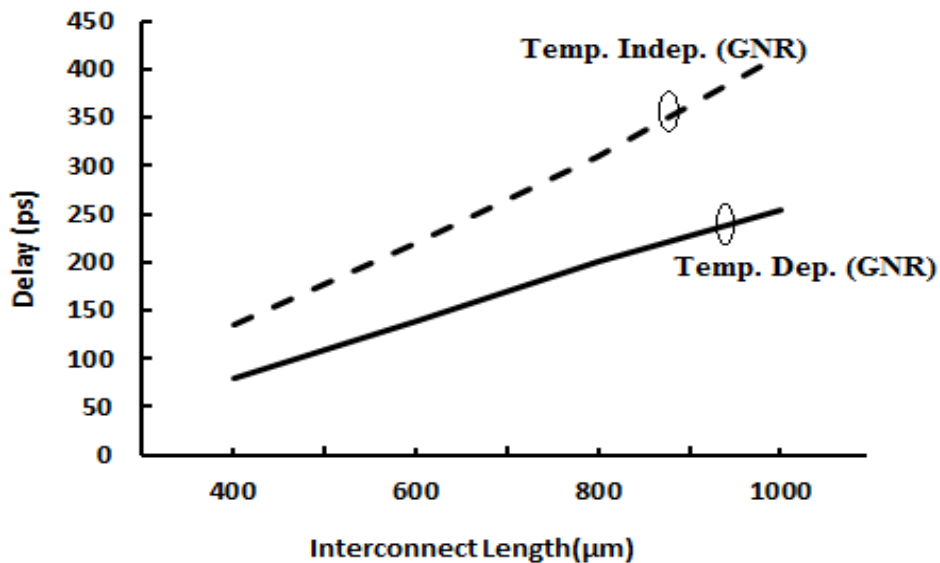


**Figure 4.5:** Temperature dependent and independent delay of MLGNR interconnects as a function of length.

Fig. 4.5 demonstrates the comparison of propagation delay between the conventionally used temperature-independent and temperature-dependent models of MLGNR interconnects. Fig. 4.5 illustrates that, the propagation delay for varied lengths, obtained through temperature-dependent models, is always smaller than the temperature-independent models of MLGNR. This is because of the substantially lower values of temperature-dependent resistance compared to temperature independent resistance over a length ranging from 400 $\mu\text{m}$  to 1000 $\mu\text{m}$  (Table 4.2).

**Table 4.3:** Average improvement in delay

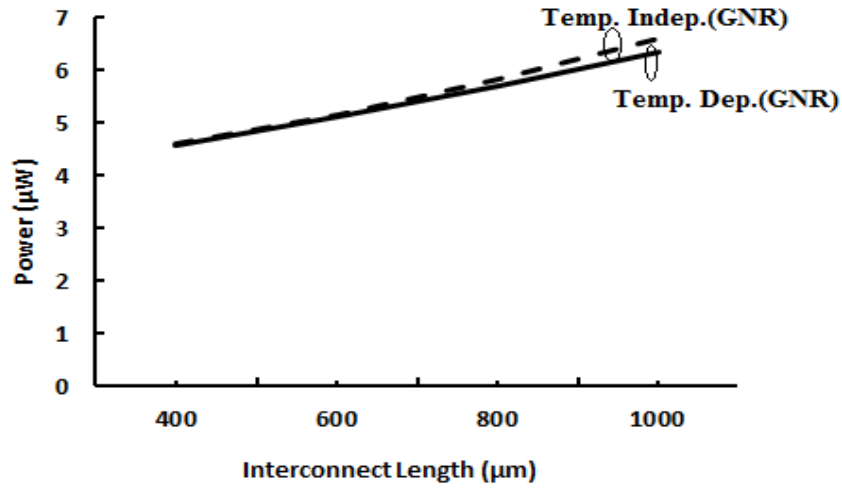
S.No.	Interconnect Length ( $\mu\text{m}$ )	Delay Improvement (%)
1	400	38.36
2	600	40.74
3	800	40.54
4	1000	72
Average Improvement		47.91

Table 4.3 shows the average improvement in propagation delay when temperature dependent model of MLGNR is used instead of the conventionally used temperature independent model. An average relative improvement of 47.91% is achieved by using temperature dependent model in comparison with temperature independent model of MLGNR.

#### 4.3.2 Power Analysis

Power dissipation is one of the main concerns in high speed integrated circuits. Power associated with interconnects increases with the aggressive technology scaling.

Fig. 4.6 illustrates the power dissipation of 1mm long interconnect of temperature dependent model of MLGNR and conventionally used temperature independent model of MLGNR at 14nm technology node. It can be observed from Fig. 4.6, that the power dissipation for varied lengths, obtained through temperature-dependent models, is comparable as compared to temperature-independent models of MLGNR. This is due to fact that the capacitance model that includes temperature-dependent channel is less sensitive to the temperature-variation.



**Figure 4.6:** Temperature dependent and independent power dissipation of MLGNR interconnects as a function of length.

Table 4.4 shows the average improvement in power dissipation when temperature dependent model of MLGNR is used instead of the conventionally used temperature independent model. An average relative improvement of 47.91% in propagation delay is achieved by using temperature dependent model in comparison with temperature independent model of MLGNR.

**Table 4.4:** Average improvement in power dissipation

S.No.	Interconnect Length (µm)	Power Dessipation Improvement (%)
1	400	0.39
2	600	1.12
3	800	2.22
4	1000	3.74
Average Improvement		1.87

### 4.3.3 Power Delay Product (PDP)

The performance of MLGNR interconnect highly depends power dissipation and delay. PDP is power delay product and is significant to the performance of MLGNR interconnect. PDP has dimension of energy and is used to measure the consumption of energy per switching

event. Fig. 4.7 illustrates the PDP of 1mm long interconnect of temperature dependent model of MLGNR and conventionally used temperature independent model of MLGNR at 14nm technology node. It can be noted from Fig. 4.7, that the PDP for varied lengths, obtained through temperature-dependent models, is less than that of temperature-independent models of MLGNR.

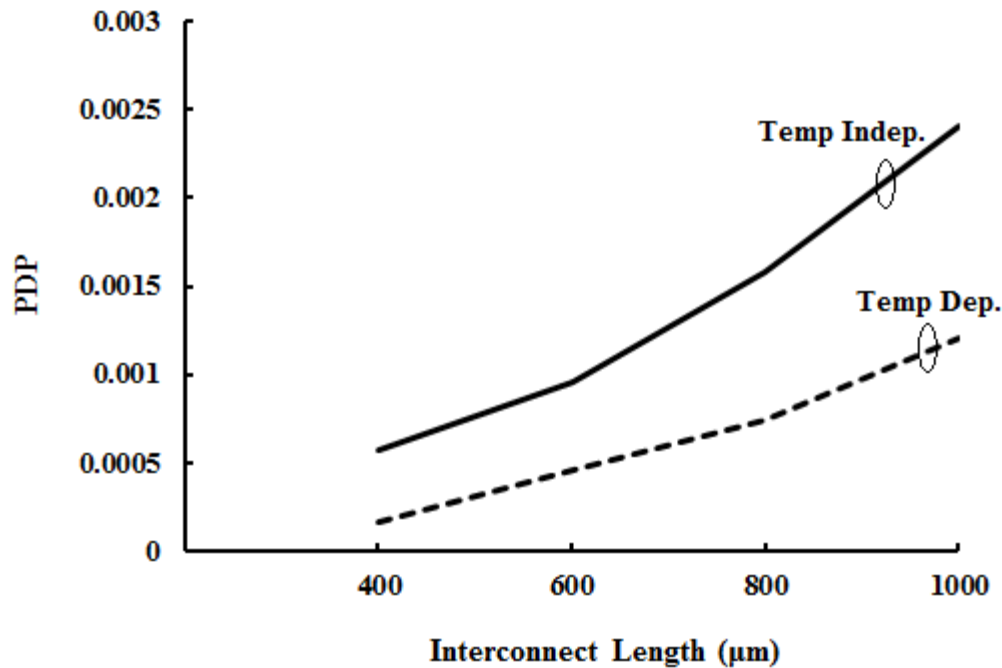


**Figure 4.7:** Temperature dependent and independent power delay product (PDP) of MLGNR interconnects as a function of length

#### 4.3.4 Frequency Spectrum Analysis

In this section the frequency spectrum of MLGNR output pulse is discussed. The frequency spectrum calculation in time domain is not always applicable due to several spectral components contained in a signal. For calculating amplitude in dB the output signal of MLGNR interconnect, is considered. The calculations are done using N point FFT (N=64) with spacing of  $f = f_s/N$  [47]. After getting FFT of the signal, its magnitude is calculated and scaled by  $1/N$ . As the spectrum is mirrored, all the useful information can be extracted by first half of the  $N/2$  values.

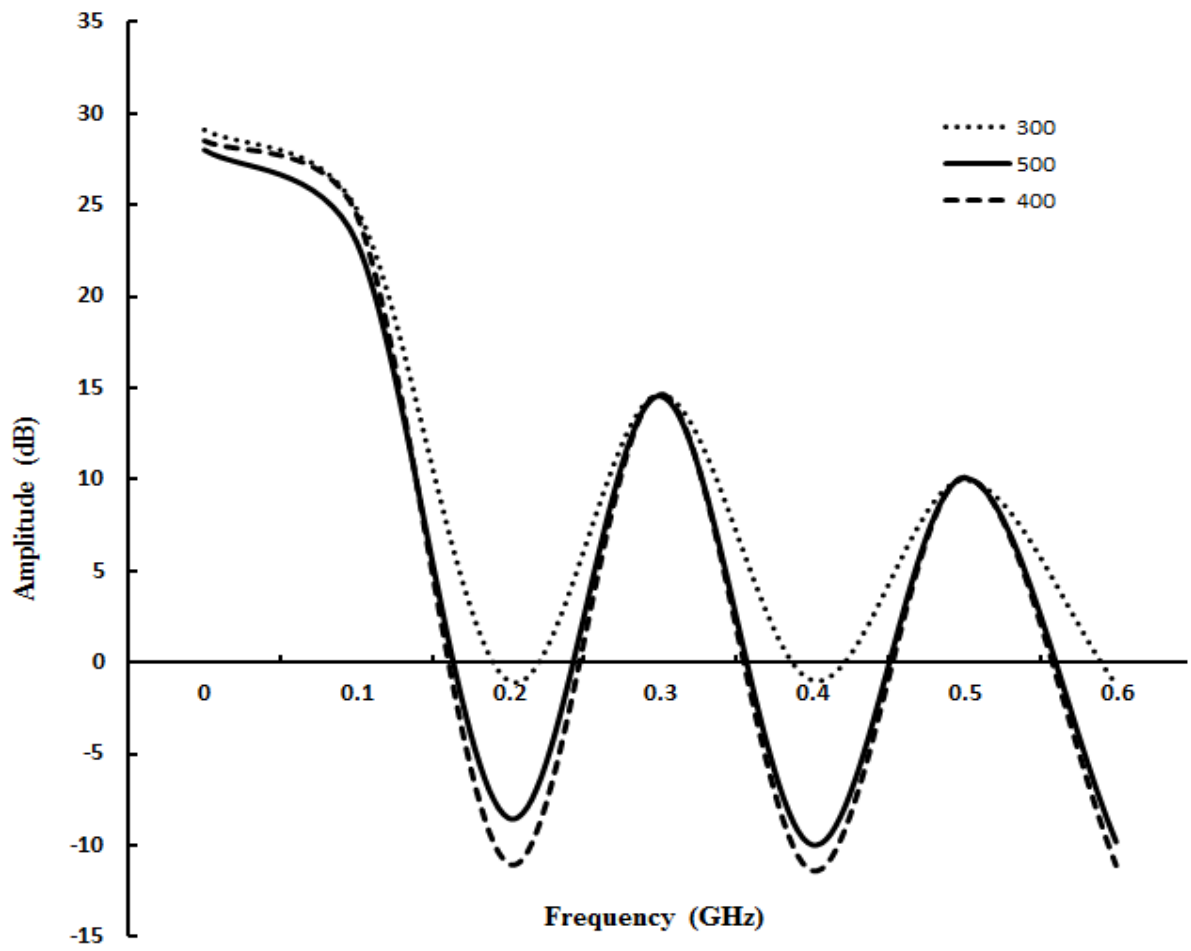


**Figure 4.8:** Frequency spectrum amplitude in dB with respect to frequency of MLGNR interconnects at different temperatures.

It can be observed by Fig. 4.8, that amplitude of the frequency spectrum waveform decreases with the increase in temperature. This reduction in amplitude causes an amplitude error known as coherent power gain (CPG), which illustrates the loss in signal power [47]. Therefore, with the increase in temperature the MLGNR interconnect lines experience more loss in signal power. Further it can also be seen that the 3-dB bandwidth of MLGNR reduces with increase in temperature. This reduction bandwidth with temperature is due to the increase in resistance with rise in temperature, shown in Fig. 4.2.

#### **4.4 CONCLUSION**

This chapter gives a detailed impedance analysis of MLGNR interconnect. It is established that MFP and no. of channels of MLGNR is sensitive to temperature and affects the value of RLC of MLGNR. Further, it is found that with the increase in temperature from 300K to 500K, the resistance of both MLGNR and Cu interconnects increases. Also, when compared with the temperature independent model, the temperature dependent model of MLGNR has lower resistance value.

This chapter also investigates the effect of temperature on delay, power and power spectrum analysis of temperature dependent and independent model of MLGNR interconnects over a temperature range from 300K to 500K at 14nm technology node. The simulation results reveal that the delay and power dissipation of MLGNR, obtained through temperature- dependent models are lower compared with conventionally (temperature-independent) used models of MLGNR, at different interconnect lengths from 400 $\mu$ m to 1000 $\mu$ m. Also the results gives the effect of temperature on the frequency spectrum of MLGNR interconnects. It is found that the increase in temperature cause the loss in signal power and decrease in bandwidth. Therefore it is important to take temperature-dependent models into consideration for high speed integrated circuits

**5.1 INTRODUCTION**

With constant scaling in technology, the feature size of chip keeps decreasing. This causes the spacing between the adjacent interconnect wires to decrease. Also, there is a significant decrease in the lateral width of interconnect wires as compared to their vertical height. Due to these cases, the coupling capacitance between the wires increases rapidly [19-22],[42]. The high performance circuits are highly temperature sensitive, therefore any type of temperature variation can cause significant effect on the crosstalk noise voltage between coupled interconnects and its frequency spectrum. Therefore, it is important to study the crosstalk induced noise voltage and its frequency spectrum between coupled MLGNR interconnects under the evidence of temperature.

This chapter explicates the effect of temperature variations on the crosstalk induced noise voltage and its frequency spectrum between coupled interconnect. Here, the crosstalk induced noise voltage at the far end of the victim line at varying temperature of 300 K to 500 K is analysed using 14nm technology node. The waveform of crosstalk induced noise voltage from the temperature dependent model and conventionally used temperature independent model are compared. An analysis is also done on the time duration of thermally aware victim line output waveforms and compared with that of the time duration of victim line output waveform of temperature independent model. Further, the variation of crosstalk amplitudes is noted at different temperature ranging from 300 K to 500 K, for varied frequencies, for MLGNR interconnect. The crosstalk amplitudes for varied frequencies of temperature dependent model are compared with the temperature independent one.

**5.2 CROSSTALK ANALYSIS**

To investigate crosstalk induced noise voltage between coupled interconnect, a capacitively coupled distributed RLC interconnects driven by CMOS inverter at 14nm technology node (as shown in Fig. 5.1) has been considered [35]. The interconnect wires are driven with the clock speed of 0.1 GHz, power supply ( $V_{dd}$ ) of 0.8V, fall time and rise time of 1ns and terminated with the capacitive load of 1fF [29, 31]. All the simulations are done using SPICE simulation

tool. For the calculation of crosstalk induced noise voltage the wire or net suffering from crosstalk noise i.e. the victim net is given logic 1 and the net that contributes to the noise i.e. the aggressor net is given a pulse switching from 1 to 0. Other simulation parameters are taken from ITRS 2012 data, shown in Table 4.1.

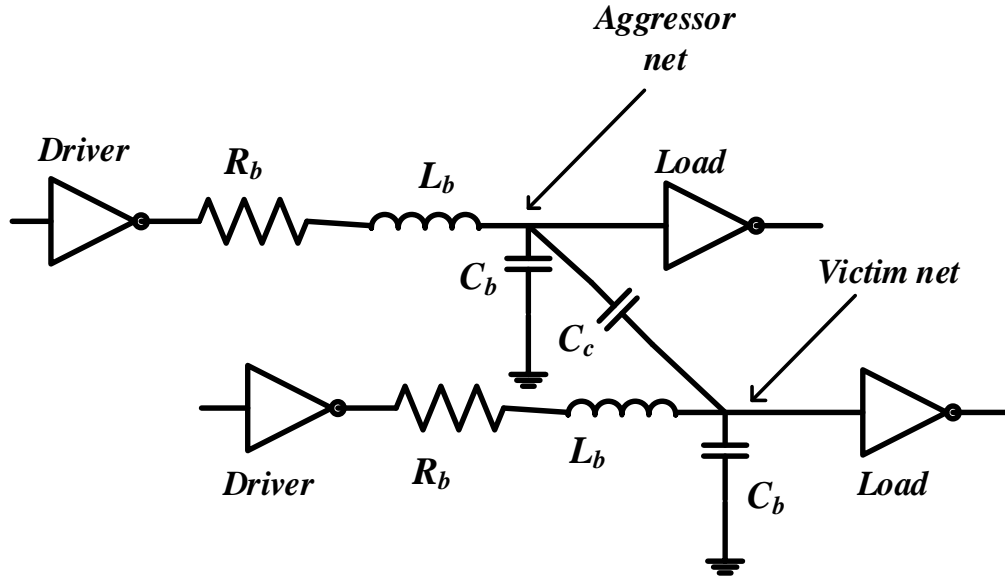


**Figure 5.1:** Capacitively coupled distributed RLC interconnects driven by CMOS inverter (driver)[22].

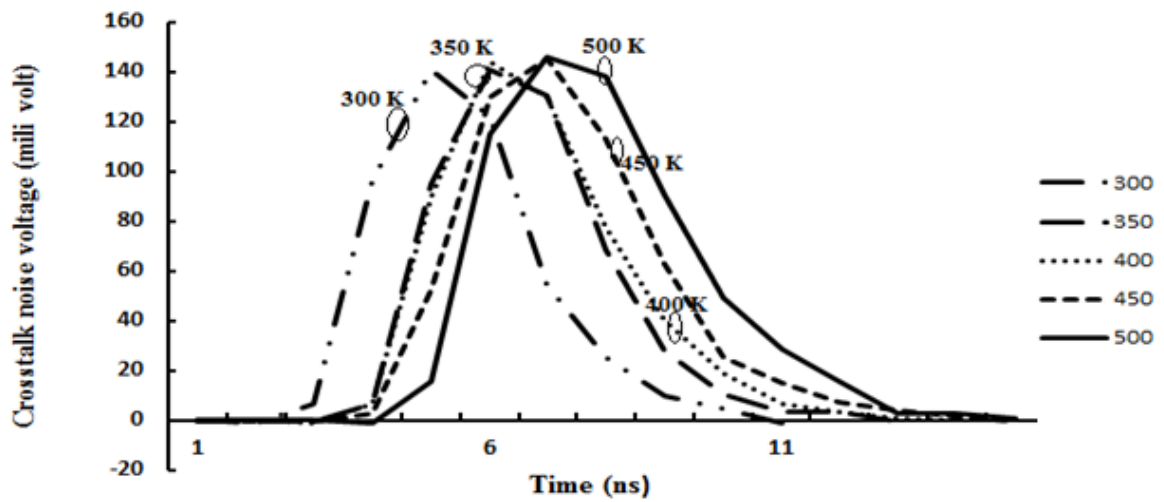


**Figure 5.2:** Temperature dependent crosstalk induced transient response of the victim output for MLGNR interconnects

Fig. 5.2 illustrates the variation in crosstalk induced transient response of the victim output at far end of the victim line due to the variation in temperature from 300K to 500K for MLGNR

bases interconnects. It is observed from Fig. 5.2, that the time duration of the crosstalk induced voltage waveform increases with increase in temperature. This is due to the dominance of increase in resistance with increase in temperature, shown in Fig. 4.2. Also, a little increase can be seen in the crosstalk noise level with the increase in temperature, this is due to the decrease in inductance of MLGNR with increase in temperature.

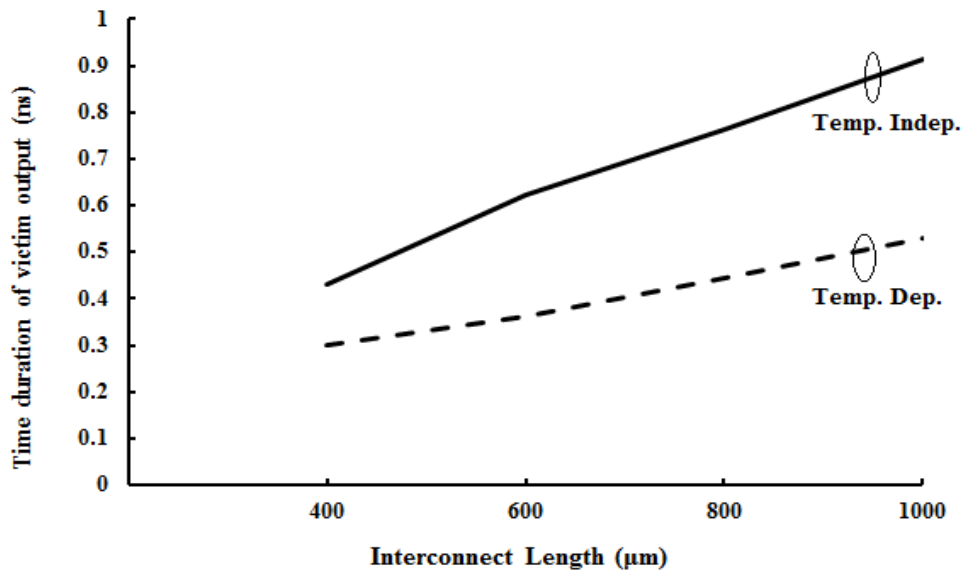


**Figure 5.3:** Variation in the time duration of output waveform of victim net for the temperature dependent and independent model of MLGNR

Fig. 5.3 illustrates the variation in the time duration of output waveform of victim net for the temperature dependent and independent model of MLGNR, with the variation of interconnect length ranging from 1000 μm to 400 μm at 14nm technology node.

It can be observed by Fig. 5.3 that the time duration of the crosstalk induced voltage waveform of temperature dependent model is less as compared to the temperature independent model, due to high resistance of temperature independent model [19].

**Table 5.1:** Average improved reduction in time duration of transient response at the victim output of temperature dependent model with that of temperature independent model.

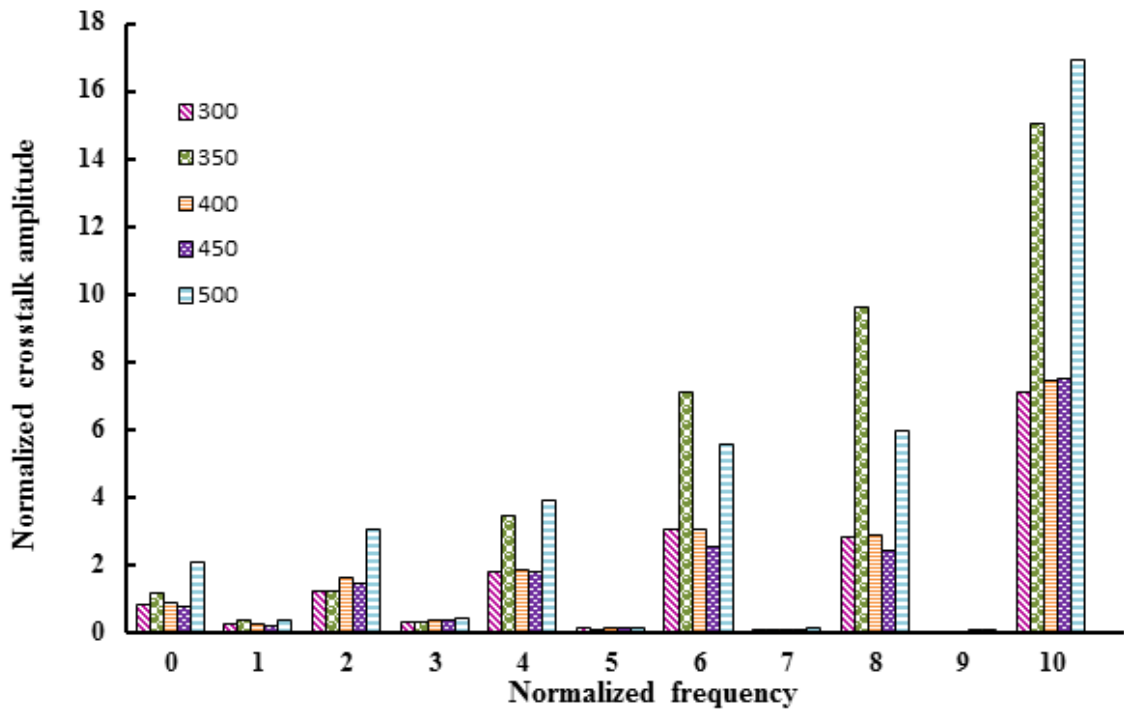
Length of interconnect ( $\mu\text{m}$ )	% improved reduction in time duration of transient response at the victim output.
400	30.09259
600	42.05457
800	41.75393
1000	42.0765
Average improvement	38.9944

Table 5.1 illustrates the average improvement in time duration when temperature dependent model is used instead of temperature independent model. It is noted that there is an average reduction of 35% in time duration of the transient response at the victim output when temperature dependent model is used instead of temperature independent model.

### 5.3 FREQUENCY SPECTRUM ANALYSIS

This chapter demonstrates the frequency spectrum analysis of the transient response of the victim output, of MLGNR interconnects. For this analysis, fast fourier transformation (FFT) technique is used to get the frequency components. The frequency components are attained using a fast fourier (FFT) program written in MATLAB. The transition period of both input and output waveforms is sampled in  $64(2^6)$  equal parts. Normalisation is done, of the amplitudes of the frequency spectrum i.e. y-axis of Fig 5.4, with that of the amplitudes of the input signal frequency. Also, the normalisation of frequencies at x-axis of Fig. 5.4 is done with the input signal frequency. Figure 5.3 shows the change in crosstalk noise levels with the change in temperature from 300K to 500K, for different frequencies.

Fig. 5.4 illustrates the variation normalised crosstalk amplitude of frequency components with the normalised signal frequency as a function of temperature variations for MLGNR. It can be observed that in the smaller frequency range there are more suppressed frequency components. Also, at all the frequencies the amplitude of crosstalk noise level generally increases.



**Figure 5.4:** Variation of normalized crosstalk amplitude of frequency components with normalized signal frequency as a function of temperature variations for MLGNR at the far end of victim line.

## 5.4 CONCLUSION

This chapter gives a detailed crosstalk analysis of MLGNR interconnects. The results show that as the temperature increases the time duration of victim output waveform also increases. Further the time duration of victim output waveform of temperature dependent model of MLGNR is compared with that of temperature independent model at different interconnect lengths, ranging from 400  $\mu\text{m}$  to 1000 $\mu\text{m}$ . An average improvement of 38.9% is noticed in the time duration of temperature dependent model of MLGNR when compared with temperature independent model.

Frequency spectrum analysis is also done on the crosstalk induced noise voltage of MLGNR and results show that at all the frequencies the amplitude of crosstalk noise level generally increases. The results also reveal that, in the smaller frequency range there are more suppressed frequency components.

**6.1 INTRODUCTION**

With the continuous scaling of technology, copper interconnect is facing some problems. With the scaling of technology in deep submicron (DSM) region, the resistance of copper interconnects has started to increase due to surface roughness and grain boundary scattering [1]-[8]. The decreased performance of copper in deep submicron (DSM) region is affecting the performance of the high performance circuits. Therefore, research is proceeding to find a better alternative of copper interconnect. In recent years, Graphene nanoribbons (GNRs) are being recommended as next generation interconnect materials [8-18]. But the thermally aware performance of MLGNR interconnects is yet to be compared with copper interconnects with the variance in temperature.

In this chapter the performance analysis in terms of propagation delay, power analysis, power delay product (PDP), frequency spectrum of output pulse, crosstalk noise and its frequency spectrum analysis of Copper interconnects is done and then compared with the results of MLGNR interconnects. This analysis is carried out for global interconnects with the variation in temperature from 300K to 500K. The results of the comparison reveal that MLGNR interconnects are better in performance as compared to copper interconnects.

**6.2 PERFORMANCE ANALYSIS AND COMPARISON OF COPPER BASED INTERCONNECTS**

All the simulation parameters are kept same for both copper and MLGNR. The simulation is performed at 14nm technology node with a clock speed of 0.1 GHz,  $V_{dd} = 0.8V$  and terminated with capacitive load of 1fF [29], [31]. For the delay, power dissipation and power delay product (PDP) analysis, same distributive *RLC* circuit of an equivalent interconnect with CMOS as a driver has been considered, as shown in Fig. 4.4. And for the crosstalk noise and

frequency spectrum analysis, the capacitively coupled distributed RLC circuit shown in Fig. 5.1 is taken.

### 6.2.1 Delay Analysis

90% propagation delay of 1mm long interconnect of MLGNR, as a function of temperature varying from 300K to 500 K at 14nm technology node, has been extracted by simulation results. Fig. 6.1 demonstrates the comparison of propagation delay between the conventionally used copper interconnects and MLGNR interconnects.

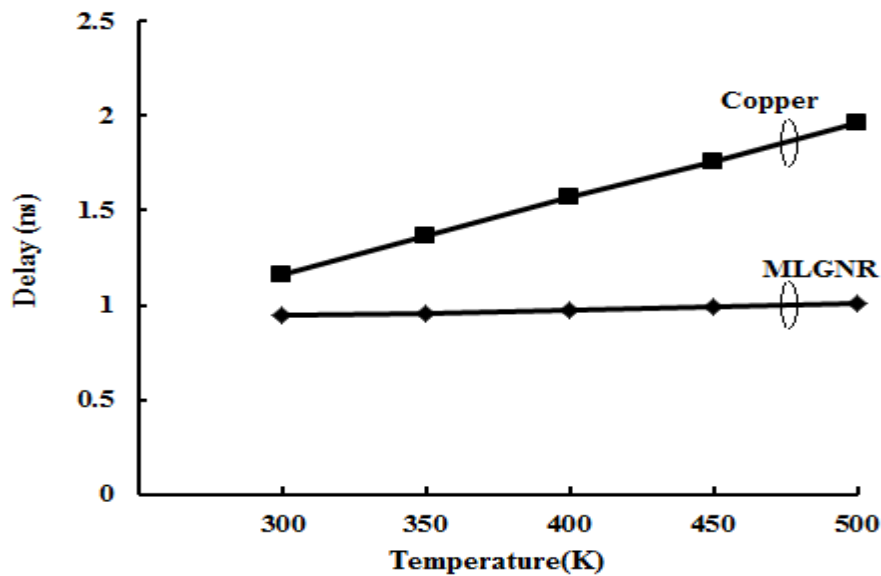


**Figure 6.1:** Temperature-dependent delay of MLGNR and copper at 14nm technology node with 1mm long interconnect.

From Fig. 6.1, it can be observed that as the temperature rises, delay of MLGNR and copper interconnects increases but this variation is observed to be more in copper. This is simply reflection of the dependency of interconnect resistance on temperature as demonstrated in Fig. 4.2.

### 6.2.2 Power dissipation Analysis

Power analysis of copper interconnects is done in the similar way as described for MLGNR interconnects. Fig. 6.2 illustrates the power dissipation of 1mm long interconnect of MLGNR and copper as a function of temperature at 14nm technology node. The power dissipation is observed to be more in copper as compared to MLGNR. This is due to higher values of resistance and capacitance associated with copper as compared to MLGNR (see Table 4.1). Also, power dissipation increases with the increases in temperature from 300K to 500 K.

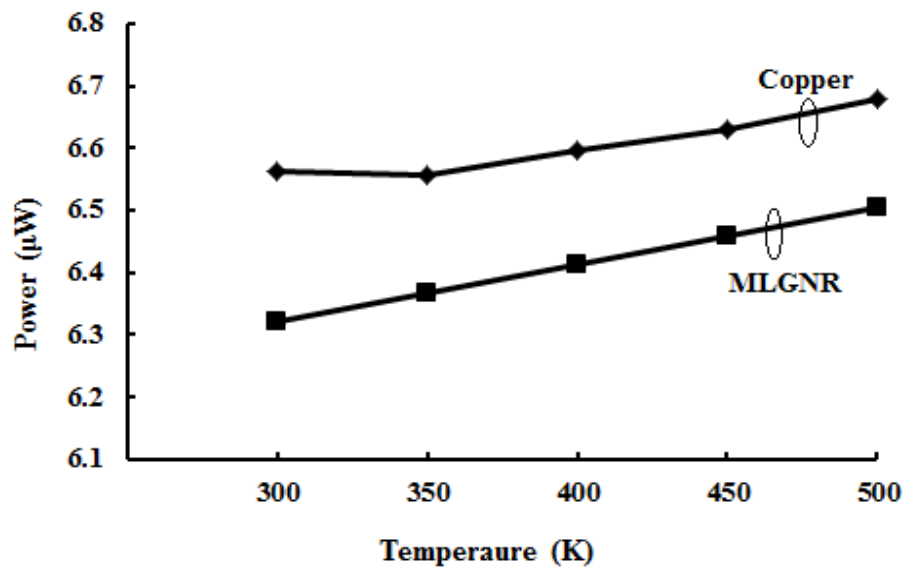


**Figure 6.2:** Temperature dependent power dissipation of MLGNR and copper at 14nm technology node with 1mm long interconnect.

### 6.2.3 Power Delay Product (PDP) Analysis

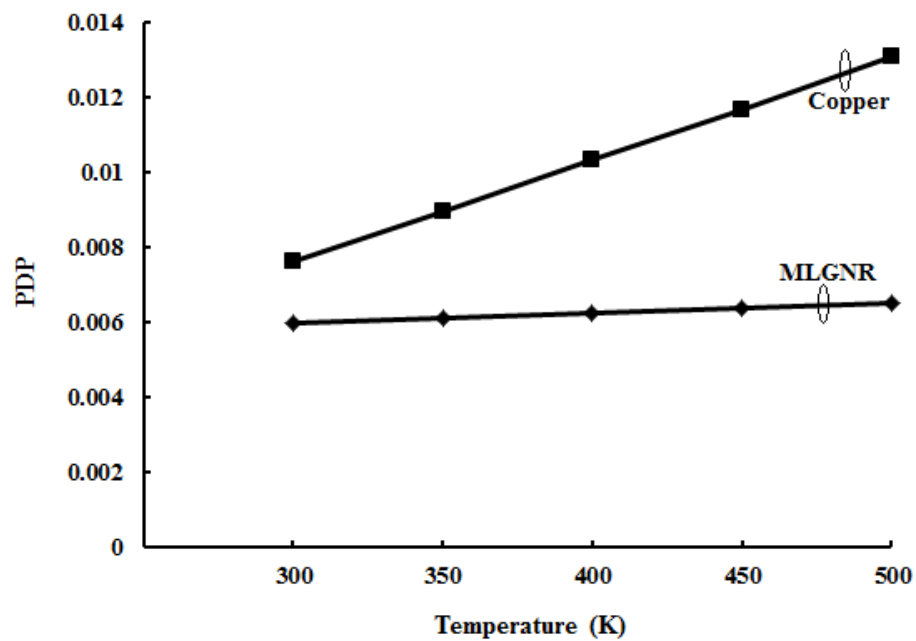


**Figure 6.3:** Power delay product (PDP) of MLGNR and copper interconnects as a function temperature.

PDP has dimension of energy and is used to measure the consumption of energy per switching event. Fig. 6.3 illustrates the PDP of 1mm long interconnect of MLGNR interconnects and conventionally used copper based interconnects at 14nm technology node. It can be noted from Fig. 6.3, that the PDP of MLGNR at varied temperature, is less than that of copper based interconnects. It can also be noted from Fig. 6.3, that PDP, irrespective of copper or MLGNR, increases with increase in temperature.

#### 6.2.4 Frequency Spectrum Analysis

The frequency spectrum in dB is calculated as explained in section 4.3.4 of chapter 4. In this section comparative analysis of frequency spectrum between copper and MLGNR is carried out. Fig. 6.4 shows the frequency spectrum in dB for both copper and MLGNR interconnects.

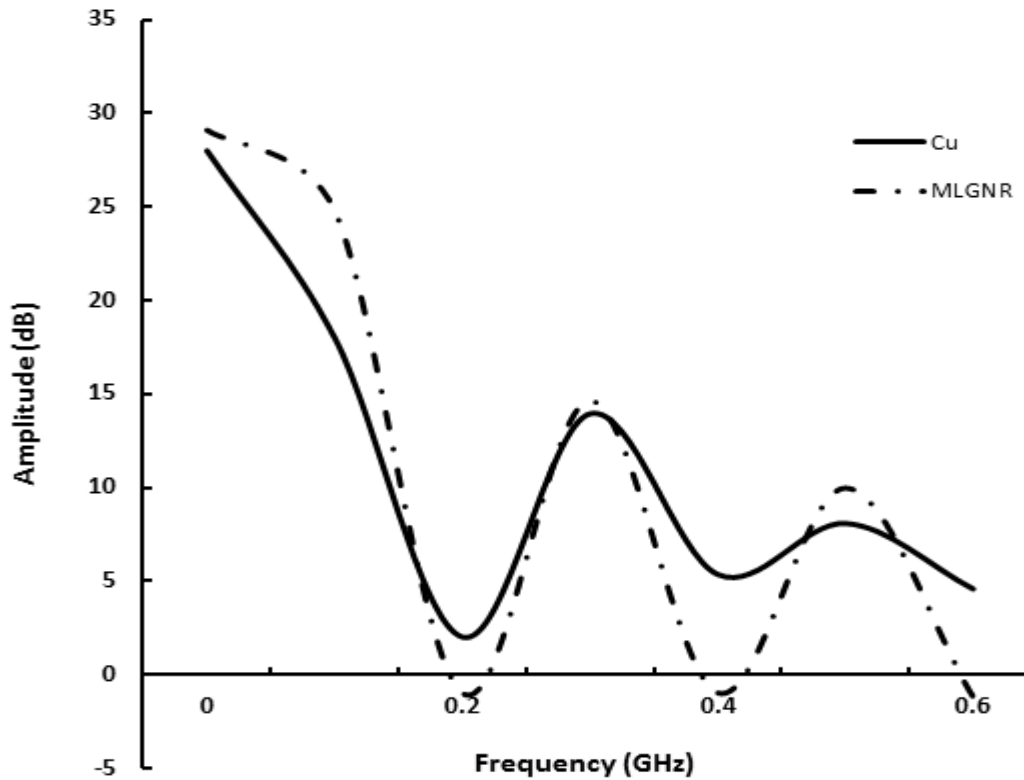


**Figure 6.4:** Frequency spectrum in dB with respect to frequency of MLGNR and Cu interconnects.

Fig. 6.4 illustrates that the 3-dB half bandwidth of MLGNR is more as compared to copper based interconnects. Table 6.1, shows the calculated 3-dB half for copper and MLGNR. Table 6.1 shows, that as compared to copper interconnects, MLGNR interconnects provides 43.5% more bandwidth. This means that MLGNR interconnects provides opportunity to retain the

half of signal power for more range of frequencies as compared to copper interconnects. Thus, MLGNR interconnects can be used in faster circuits as compared to copper based interconnects

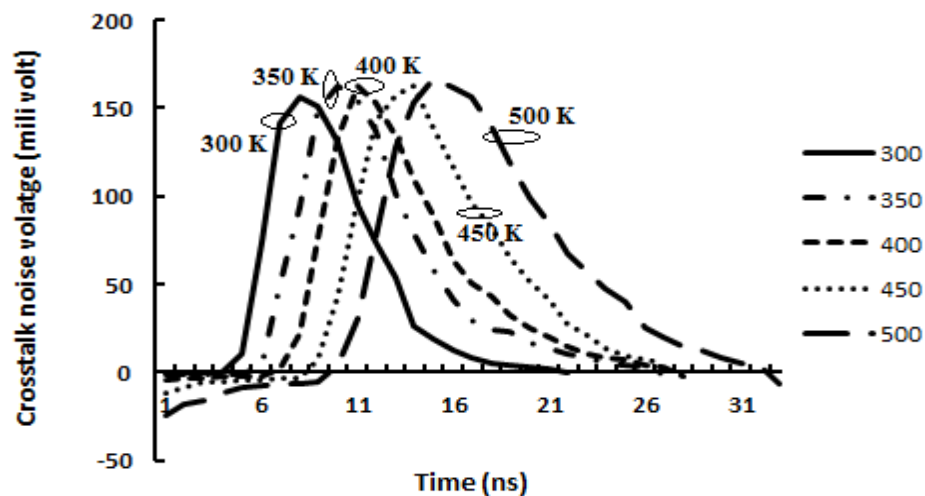
**Table 6.1:** Improvement (%) in bandwidth of MLGNR as compared to Cu

Interconnect	3-dB half bandwidth
MLGNR	0.124
Cu	0.07
(%) Improvement	43.5%

### 6.2.4 Crosstalk Analysis

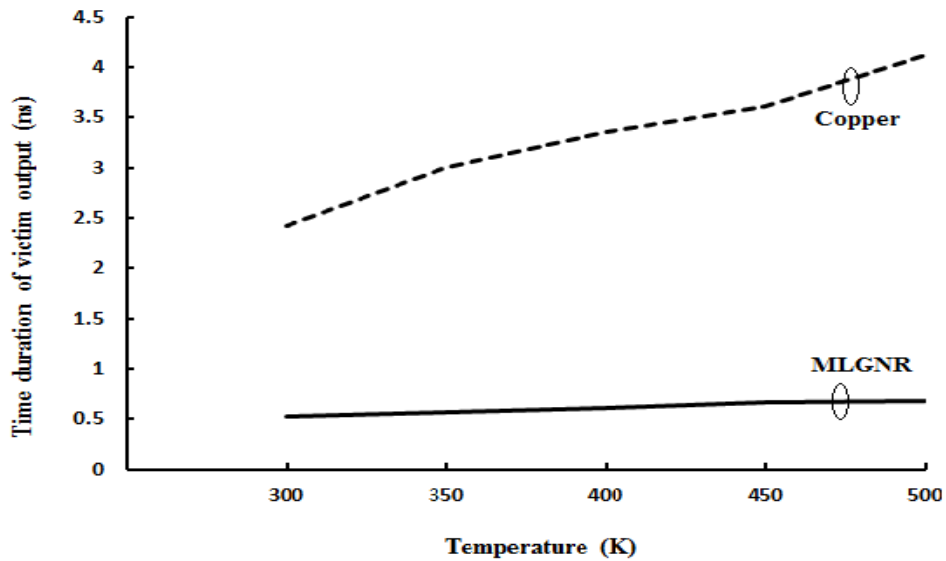
To analyse crosstalk in copper based interconnects, a capacitively coupled distributed RLC interconnects driven by CMOS inverter at 14nm technology node (as shown in Fig. 5.1). All the simulation parameters are taken same as in the crosstalk analysis of MLGNR. For the calculation of crosstalk induced noise voltage the wire or net suffering from crosstalk noise i.e. the victim net is given logic 1 and the net that contributes to the noise i.e. the aggressor net is given a pulse switching from 1 to 0.

Fig. 6.5 illustrates the variation in crosstalk induced transient response of the victim output at far end of the victim line due to the variation in temperature from 300K to 500K for copper bases interconnects. It is observed from Fig. 6.6, that the time duration of the crosstalk induced voltage waveform increases with increase in temperature.



**Figure 6.5:** Temperature dependent crosstalk induced transient response of coupled interconnects.

A comparative analysis is done between the time duration of copper based interconnects and MLGNR interconnect over different temperature from 300 K to 500 K, shown Fig. 6.6.



**Figure 6.6:** Variation in the time duration of output waveform of victim net of MLGNR and copper at different temperatures from 300K to 500K.

Table 6.2 shows the average improvement in time duration of MLGNR when compared to copper interconnects. It can be observed from Table 6.2, that there is an average improvement of 81.14% in time duration of MLGNR as compared to copper based interconnects.

**Table 6.2:** Average improved reduction in time duration of transient response at the victim output of MLGNR with that copper interconnects.

Length of interconnect ( $\mu\text{m}$ )	% improved reduction in time duration of transient response at the victim output.
300	78.0992
350	80.9
400	81.8452
450	81.4127
500	83.4223
Average	81.1359

### 6.2.5 Frequency Spectrum Analysis

The frequency components of crosstalk noise voltage are obtained using FFT program written MATLAB with transition time of input and output sampled in  $64(2^6)$  equal parts. The y-axis i.e. amplitudes of the frequency spectrum is normalised by amplitudes of the input signal frequency and x-axis i.e. frequencies are normalised by input signal frequency. Fig. 6.7 shows the change in crosstalk noise levels of copper interconnects with the change in temperature from 300K to 500K, for different frequencies.

Fig. 6.7 and Fig. 5.4, reveals that for the whole range of normalised frequency, with the rise in temperature, the amplitude levels of noise in MLGNR is less than copper and filter more noise components of victim output. Also, the noise frequency components are more suppressed in smaller frequency range for both MLGNR and copper based interconnects.

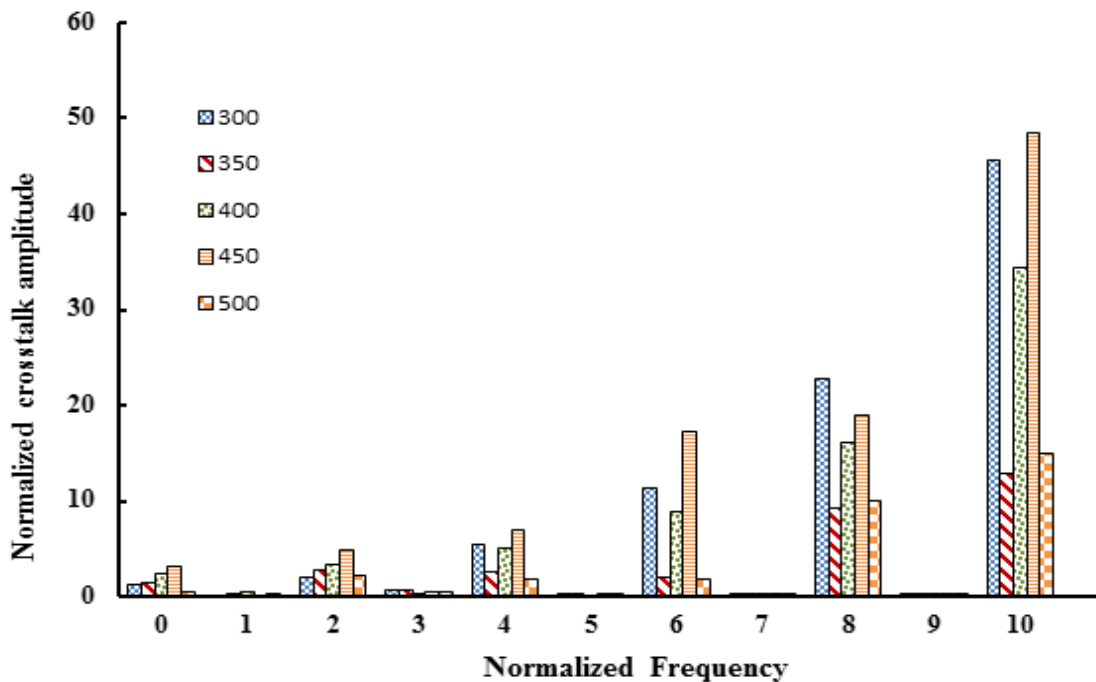


**Figure 6.7:** Variation of normalized crosstalk amplitude of frequency components with normalized signal frequency as a function of temperature variations for copper at the far end of victim line.

### **6.3 CONCLUSION**

This chapter gives a detailed performance analysis of copper interconnects in terms of signal delay, power dissipation, frequency spectrum of output pulse, crosstalk and its frequency spectrum. The results are then compared with the results of MLGNR interconnects. For delay analysis the results reveal that as the temperature rises, delay of MLGNR and copper interconnects increases but this variation is observed to be more in copper. Also, power dissipation and PDP is spectrum observed to be more in copper as compared to MLGNR. Further in the chapter frequency analysis is done and it is observed that the loss in signal power is more in the case of copper interconnects as compared to MLGNR interconnects. Also, it is noticed that MLGNR interconnects can be used in faster circuits as compared to copper based interconnects.

Last two sections cover the crosstalk and its frequency spectrum analysis. The results reveal that for both MLGNR and copper interconnects the time duration of the crosstalk induced voltage waveform increases with increase in temperature but there is average reduction of 81.14% in time duration of MLGNR with that of copper based interconnects. Further it is revealed frequency analysis, that the amplitude levels of noise in MLGNR is less than copper and filter more noise components of victim output.

**7.1 INTRODUCTION**

With the continuous scaling of technology, copper interconnect is facing some problems. With the scaling of technology in deep submicron (DSM) region, the resistance of copper interconnects has started to increase due to surface roughness and grain boundary scattering [1]-[8]. The decreased performance of copper in deep submicron (DSM) region is affecting the performance of the high performance circuits. Also, it is seen that variation in temperature impacts the performance of interconnects in terms of delay, power and crosstalk. These are the main parameters that limit the performance of copper in deep submicron technology node. Therefore, there is a need to introduce an alternative material for VLSI interconnects.

This chapter includes the concluding remarks of the work given in previous chapters. It is found that with the variation in temperature from 300K to 500K, MLGNR presents to be a good alternative material compared to copper based interconnects.

**7.2 SUMMARY**

**Chapter 1** gives an overview about the thesis and presents its objective and organization.

**Chapter 2** of the thesis briefly explains and discusses the previously done work on the topic of interconnects. With the scaling of technology the performance degradation in copper is briefly studied. Many researchers proposed carbon nanotubes (CNTs) and multilayer graphene nanoribbons (MLGNRs) as possible alternatives for Cu in future. Many researchers recommended GNRs as a future interconnect material and transistors due to its easily controlled structure.

**Chapter 3** presents temperature dependent modeling of MLGNR based interconnects. Also, the modeling of copper based interconnects is presented in the same chapter. The RLC parameters of both MLGNR and copper based interconnects are used for performance analysis. Side contact MLGNR is taken for performance analysis due to its less resistance value compared to top contact MLGNR.

**Chapter 4** gives a brief temperature dependent impedance and performance analysis, in terms of propagation delay, power dissipation and frequency spectrum, of MLGNR with smooth edges. It was observed that the mean free path and number of conducting channels are temperature dependent variables. It was found that resistance of both MLGNR and copper increases with increase in temperature. The RLC parameters of MLGNR and copper are calculated at global lengths ranging from 400  $\mu\text{m}$  to 1000 $\mu\text{m}$  and over the range of 300K to 500K at 14 nm technology. It is found that the impedance values of MLGNR are less than that of copper based interconnects. Also the impedance values of thermally aware model of MLGNR are found to be less than temperature independent model.

Further in the chapter performance analysis of MLGNR in terms of delay, power dissipation, PDP and frequency spectrum of the output pulse is done using temperature dependent model and compared with conventionally used temperature independent model. It was found that the simulation results reveal that the delay and power dissipation of MLGNR, obtained through temperature dependent models are lower compared with conventionally (temperature-independent) used models of MLGNR. It was also discovered that the increase in temperature cause the loss in signal power and decrease in bandwidth. Therefore it is important to take temperature dependent models into consideration for high speed integrated circuits.

**Chapter 5** presents the brief analysis of crosstalk induced noise in MLGNR based interconnects. Results show that as the temperature increases the time duration of victim output waveform also increases. Further the time duration of victim output waveform of temperature dependent model of MLGNR is compared with that of temperature independent model at different interconnect lengths, ranging from 400  $\mu\text{m}$  to 1000 $\mu\text{m}$ . An average improvement of 38.9% is noticed in the time duration of temperature dependent model of MLGNR when compared with temperature independent model. Further, frequency spectrum analysis is also done on the crosstalk induced noise voltage of MLGNR and results show that at all the frequencies the amplitude of crosstalk noise level generally increases. The results also reveal that, in the smaller frequency range there are more suppressed frequency components.

**Chapter 6** gives a detailed performance analysis of copper interconnects in terms of signal delay, power dissipation, frequency spectrum of the output pulse, crosstalk induced noise voltage and its frequency spectrum. The results are then compared with the results of MLGNR interconnects. For the delay, power and PDP analysis the results reveal that as the temperature

rises, delay, power dissipation and PDP of MLGNR and copper interconnects increases but this variation is observed to be more in copper. Further in the chapter frequency spectrum analysis of output is done and it is observed that MLGNR interconnects can be used in faster circuits as compared to copper based interconnects.

For the crosstalk and its frequency spectrum analysis, the results reveal that for both MLGNR and copper interconnects the time duration of the crosstalk induced voltage waveform increases with increase in temperature but there is average reduction of 81.14% in time duration of MLGNR with that of copper based interconnects. Further it is revealed in frequency analysis, that the amplitude levels of noise in MLGNR is less than copper and filter more noise components of victim output.

### **7.3 FUTURE WORK**

In this study, it is been observed that MLGNR based interconnects, due to its high current density and high mean free path, can be implemented as a part of a VLSI circuit instead of copper based interconnects at 14 nm technology, in order to reduce power, PDP, delay and the crosstalk noise voltage. Some suggestions for future work in the fields of MLGNR interconnects are given below:

- MLGNRs face a problem of edge roughness which deteriorates its performance. Therefore, there is a need for work to be done to improve the fabrication techniques.
- Performance of MLGNRs is yet not compared with mixed carbon nanotube bundle (MCB) interconnects, which are also considered to be possible material to replace copper based interconnects.

## REFERENCES

---

- [1] W.Steinhogl, et al, "Comprehensive study of the resistivity of copper wires with lateral dimensions of 100nm and smaller," *Journal of Applied Physics*,vol.97,pp. 023706(1-7), 2005.
- [2] A. Naeemi, R. Sarvari, and J.D. Meindl, "Performance comparison between carbon nanotube and copper interconnects for giga scale integration (GSI)", *Electron Device letters*, vol. 26, No. 2, pp. 84-86, 2005.
- [3] F. Kreupl, et al, "Carbon nanotubes in interconnect applications." *Microelectronic Engineering*,vol. 64, no. 1, pp.399-408,2002.
- [4] Hong Li, W. Y. Yin, Kaustav Banerjee, and Jun-Fa Mao. "Circuit modeling and performance analysis of multi-walled carbon nanotube interconnects." *IEEE Transactions on electron devices*, vol. 55, no. 6, pp.1328-1337, 2008.
- [5] M.K. Rai and S. Sarkar. "Influence of tube diameter on carbon nanotube interconnect delay and power output." *physica status solidi (a)* vol. 208, no. 3, pp.735-739, 2011.
- [6] N. Srivastava and K. Banerjee. "Performance analysis of carbon nanotube interconnects for VLSI applications." In *Proceedings of the 2005 IEEE/ACM International conference on Computer-aided design*, IEEE Computer Society, pp. 383-390, 2005.
- [7] M. K. Rai., B. K. Kaushik., and S. Sarkar. "Thermally aware performance analysis of single-walled carbon nanotube bundle as VLSI interconnects". *Journal of Computational Electronics*, vol. 15, no.2, pp.407-419, 2016.
- [8] M. K. Rai, et al., "Performance analysis of multilayer graphene nanoribbon (MLG NR) interconnects." *Journal of Computational Electronics*, vol.15, no. 2, pp.358-366, 2016.
- [9] Y.W. Tan, et al. "Measurement of scattering rate and minimum conductivity in graphene." *Physical review letters*, vol.99, no.24, p.246803, Dec. 2007.
- [10] A. Naeemi and J. D. Meindl. "Performance benchmarking for graphene nanoribbon, carbon nanotube, and Cu interconnects." *IEEE Proc. on International Interconnect Technology Conference, (IITC 2008)*. pp. 183-185. IEEE, 2008

- [11] A.K. Gei, and K.S. Novoselov. "The rise of graphene." *Nature materials*. vol. 6, no. 3, pp.183-191, 2007.
- [12] S. Rakheja, V. Kumar, and A. Naeemi. "Evaluation of the potential performance of graphene nanoribbons as on-chip interconnects." *Proceedings of the IEEE*, vol.101, no. 7, pp.1740-1765, 2013
- [13] R. Van Noorden, "Moving towards a graphene world," *Nature*, vol. 442, no. 7100, pp. 228–229,2006.
- [14] A.K. Nishad, R. Sharma. "Analytical Time-Domain Models for Performance Optimization of Multilayer GNR Interconnects." *IEEE J. Sel. Top. Quantum Electronics*, vol.20, no. 1, pp.17-24, 2014.
- [15] V.R. Kumar et al, "Time and Frequency Domain Analysis of MLGNR Interconnects." *IEEE Transactions on Nanotechnology*, vol. 14, no. 3 ,pp.484-492, 2015.
- [16] A. A. Balandin, et al, "Superior thermal conductivity of single-layer graphene." *Nano letters*, vol.8, no. 3, pp.902-907, 2008.
- [17] X. Chuan, H. Li and K. Banerjee. "Modeling, analysis, and design of graphene nano-ribbon interconnects." *IEEE transactions on electron devices*, vol.56, no.8, pp. 1567-1578,2009.
- [18] H. Li, et al,. "Carbon nanomaterials for next-generation interconnects and passives: physics, status, and prospects." *IEEE Transactions on Electron Devices*, vol.56, no. 9, pp.1799-1821, 2009.
- [19] M.K. Rai, and S. Sarkar, "Temperature dependant crosstalk analysis in coupled single-walled carbon nanotube (SWCNT) bundle interconnects," *International Journal of Circuit Theory and Applications*, vol.43, no.10, pp.1367-1378, 2015.
- [20] B.K. Kaushik, and S Sarkar, "Crosstalk analysis for a CMOS-gate-driven coupled interconnects," *IEEE Transactions on Computer-Aided Design of Integrated Circuits and Systems*, Vol.27, no.6, pp.1150-1154, June 2008.
- [21] S.N. Pu, W.Y. Yin, J.F. Mao, and Q.H. Liu, "Crosstalk prediction of single-and double-walled carbon-nanotube (SWCNT/DWCNT) bundle interconnects," *IEEE Transactions on Electron Devices*, vol.56, no.4, pp.560-568, April 2009.

- [22] D Das, and H Rahaman, "Analysis of crosstalk in single-and multiwall carbon nanotube interconnects and its impact on gate oxide reliability," *IEEE Transactions on Nanotechnology*, vol.10, no.6, pp.1362-1370, Nov. 2011.
- [23] V. Kumar, S. Rakheja and A. Naeemi. "Modeling and optimization for multi-layer graphene nanoribbon conductors." In *Interconnect Technology Conference and 2011 Materials for Advanced Metallization (IITC/MAM), 2011 IEEE International*. pp. 1-3, May 2011.
- [24] W.S. Zhao and W.Y. Yin. "Comparative study on multilayer graphene nanoribbon (MLG NR) interconnects." *IEEE Transactions on Electromagnetic Compatibility*, vol.56, no.3, pp.638-645, 2014.
- [25] V. Kumar, S. Rakheja and A. Naeemi. "Performance and energy-per-bit modeling of multilayer graphene nanoribbon conductors." *IEEE transactions on electron devices*. Vol.59, no.10, pp.2753-2761, 2012.
- [26] C. Xu, H. Li and K. Banerjee. "Graphene nano-ribbon (G NR) interconnects: A genuine contender or a delusive dream?." In *Electron Devices Meeting, 2008. IEDM 2008. IEEE International* , pp. 1-4, December 2008.
- [27] T. Ragheb and Y. Massoud. "On the modeling of resistance in graphene nanoribbon (G NR) for future interconnect applications." *Proceedings of the 2008 IEEE/ACM International Conference on Computer-Aided Design*. IEEE Press, November 2008.
- [28] V. Kumar, S. Rakheja and A. Naeemi. "Review of multi-layer graphene nanoribbons for on-chip interconnect applications." In *Electromagnetic Compatibility (EMC), 2013 IEEE International Symposium on*, pp. 528-533, August 2013.
- [29] V.R. Kumar, M.K. Majumder, N.R. Kukkam and B.K. Kaushik. "Time and frequency domain analysis of MLG NR interconnects." *IEEE Transactions on Nanotechnology*.vol.14 no.3, pp.484-492, 2015
- [30] A.G. Chiariello, A. Maffucci, and G .Miano. "A temperature-dependent circuit model for carbon-based on-chip global interconnects." *2012 12th IEEE Conference on Nanotechnology (IEEE-NANO)*, pp. 1-6, August 2012.

- [31] E.H. Hwang, S. Adam, and S.D. Sarma. "Carrier transport in two-dimensional graphene layers." *Physical review letters*, vol. 98, no.18, p.186806, 2007.
- [32] Hosseini A, Shabro V. "Thermally-aware modeling and performance evaluation for singlewalled carbon nanotube-based interconnects for future high performance integrated circuits." *Microelectronic Engineering*, vol. 87, no. 10, pp.1955–1962,2010.
- [33] A. Maffucci and G. Miano . "Number of conducting channels for armchair and zig-zag graphene nanoribbon interconnects." *IEEE transactions on nanotechnology*. vol 12, no. 5, pp.817-823, 2013.
- [34] Eric Pop, David A. Mann, Kenneth E. Goodson, and Hongjie Dai. "Electrical and thermal transport in metallic single-wall carbon nanotubes on insulating substrates." *Journal of Applied Physics* 101, no. 9, p.093710(1-11), 2007.
- [35] Y. Fang, et al. "Circuit modelling of multilayer graphene nanoribbon (MLGNR) interconnects." In *Electromagnetic Compatibility (APEMC), 2012 Asia-Pacific Symposium on*, pp. 625-628, May 2012
- [36] SH Nasiri, R. Faez. "Compact formulae for number of conduction channels in various types of graphene nanoribbons at various temperatures." *Mod. Phys. Lett. B.*, vol. 26, no. 1, pp.1-5, 2012.
- [37] A.Naeemi and J.D. Meindl. "Compact physics-based circuit models for graphene nanoribbon interconnects." *IEEE Transactions on Electron Devices*, vol.56, no.9, pp.1822-1833,2009
- [38] D.A. Areshkin, D. Gunlycke, and C.T.White. "Ballistic transport in graphene nanostrips in the presence of disorder: Importance of edge effects." *Nano letters*, vol. 7, no.1, pp.204-210, 2007.
- [39] M.K. Rai and S. Sarkar. "Influence of distance between adjacent tubes on SWCNT bundle interconnect delay and power dissipation." *Journal of Computational Electronics*, vol.12, no.4, pp.796-802, 2013

- [40] H. Kempa, P. Esquinazi and Y. Kopelevich,. "Field-induced metal-insulator transition in the c-axis resistivity of graphite." *Physical Review B*, vol.65, no.24, p.241101, 2002
- [41] Sungjun Im, Navin Srivastava, Kaustav Banerjee, and Kenneth E. Goodson. "Scaling analysis of multilevel interconnect temperatures for high-performance ICs." *IEEE Transactions on Electron Devices* 52, no. 12, pp. 2710-2719, 2005.
- [42] S.C.Wong, G.Y. Lee, and D.J. Ma. "Modeling of interconnect capacitance, delay, and crosstalk in VLSI." *IEEE Transactions on semiconductor manufacturing*, vol. 13, no.1, pp.108-111, 2000
- [43] Predictive technology model (PTM)[Online], <http://ptm.asu.edu/>.
- [44] Semiconductor Industry Association, International Technology Roadmap for Semiconductors (ITRS), 2012 update, [Online]. Available:<http://www.itrs.net/>
- [45] R. Chandel, S. Sarkar, and R. P. Agarwal. "Delay, management. power, voltage-scaled. of driven repeater, interconnects. long." *Int. J. Model. Simul.*, vol. 27,p.333339, 2007
- [46] M.A. El-Moursy, and E.G. Friedman. "Power characteristics of inductive interconnect." *IEEE Transactions on Very Large Scale Integration (VLSI) Systems*. vol. 12, no. 12, pp.1295-1306, 2004.
- [47] S. Scholl. "Exact Signal Measurements using FFT Analysis", 2016

% **16**  
SIMILARITY INDEX

% **1**  
INTERNET SOURCES

% **16**  
PUBLICATIONS

% **0**  
STUDENT PAPERS

---

PRIMARY SOURCES

---

**1** Rai, Mayank Kumar, and Sankar Sarkar. "Temperature dependant crosstalk analysis in coupled single-walled carbon nanotube (SWCNT) bundle interconnects : COUPLED SWCNT BUNDLE INTERCONNECTS PERFORMANCE", International Journal of Circuit Theory and Applications, 2014. **%3**

Publication

---

**2** Rai, Mayank Kumar, Brajesh Kumar Kaushik, and Sankar Sarkar. "Thermally aware performance analysis of single-walled carbon nanotube bundle as VLSI interconnects", Journal of Computational Electronics, 2016. **%2**

Publication

---

**3** Mayank Kumar Rai, Harsh Garg, B. K. Kaushik. "Temperature-Dependent Modeling and Crosstalk Analysis in Mixed Carbon Nanotube Bundle Interconnects", Journal of Electronic Materials, 2017. **%2**

Publication

---

Rai, Mayank Kumar, Ashoke Kumar Chatterjee,

4

Sankar Sarkar, and B. K. Kaushik.  
"Performance analysis of multilayer graphene nanoribbon (MLG NR) interconnects", Journal of Computational Electronics, 2016.

Publication

%2

5

SpringerBriefs in Applied Sciences and Technology, 2016.

Publication

%1

6

Kumar, Vachan, Shaloo Rakheja, and Azad Naeemi. "Performance and Energy-per-Bit Modeling of Multilayer Graphene Nanoribbon Conductors", IEEE Transactions on Electron Devices, 2012.

Publication

%1

7

Mayank, , and Sankar Sarkar. "Carbon Nanotube as a VLSI Interconnect", Electronic Properties of Carbon Nanotubes, 2011.

Publication

%1

8

Yajun Ha. "Fast and Accurate Interval-Based Timing Estimator for Variability-Aware FPGA Physical Synthesis Tools", 2007 International Conference on Field Programmable Logic and Applications, 08/2007

Publication

%1

9

Kumar, Mekala Girish, Yash Agrawal, and Rajeevan Chandel. "Carbon Nanotube Interconnects – A Promising Solution for VLSI

%1